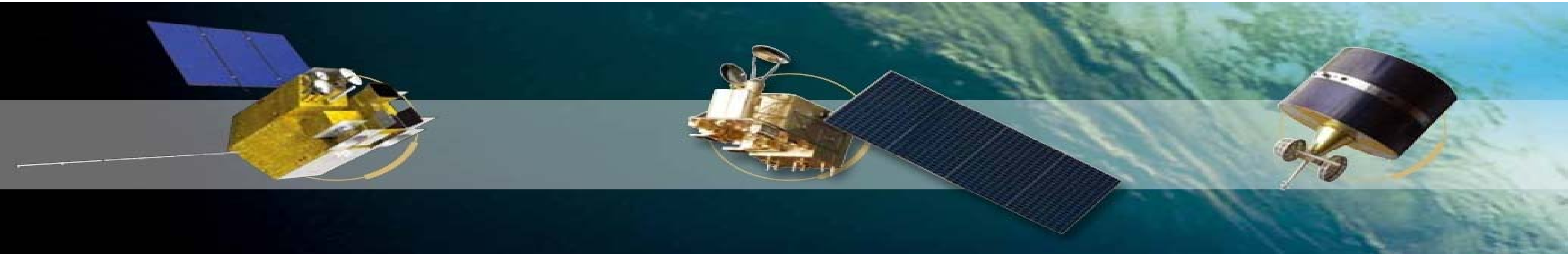

# RTTOV Performance Evaluation


Ma Gang

National Satellite Meteorological Center


30，Apr. 2019

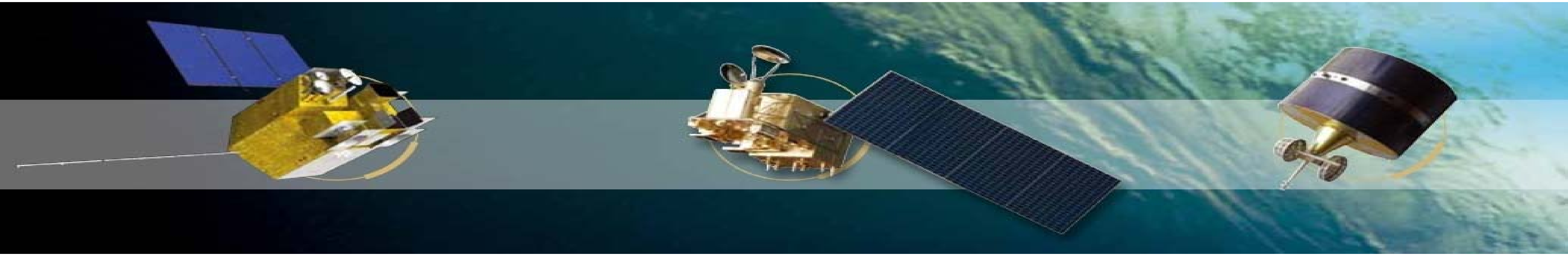

- Fast Radiative Transfer Model
- RTTOV to FY satellite
- Pre-Quality Control to assimilation of FY Data
- Summery
- Program in future

# Fast Radiative Transfer Model

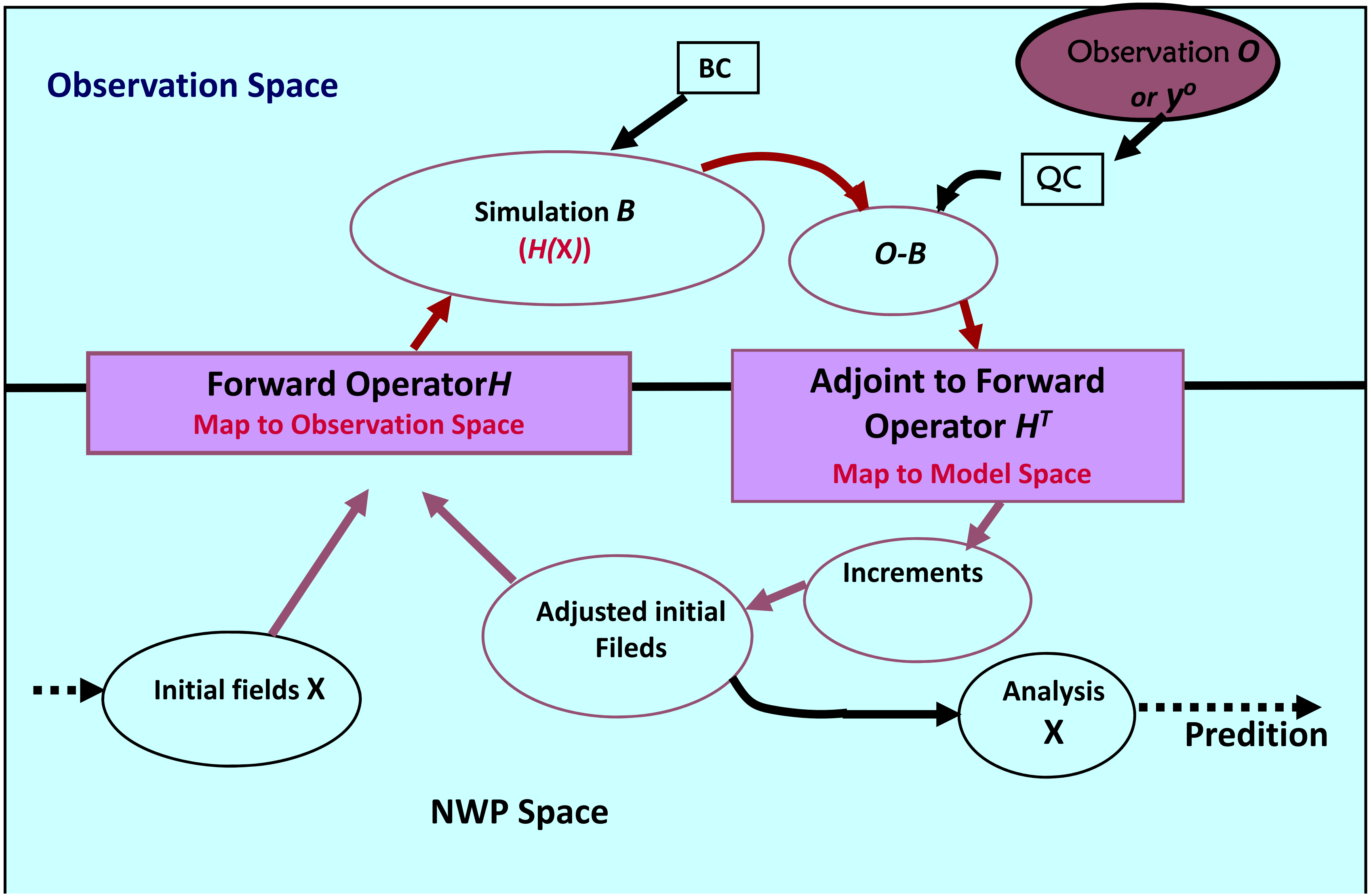

# Fast Radiative Transfer Model

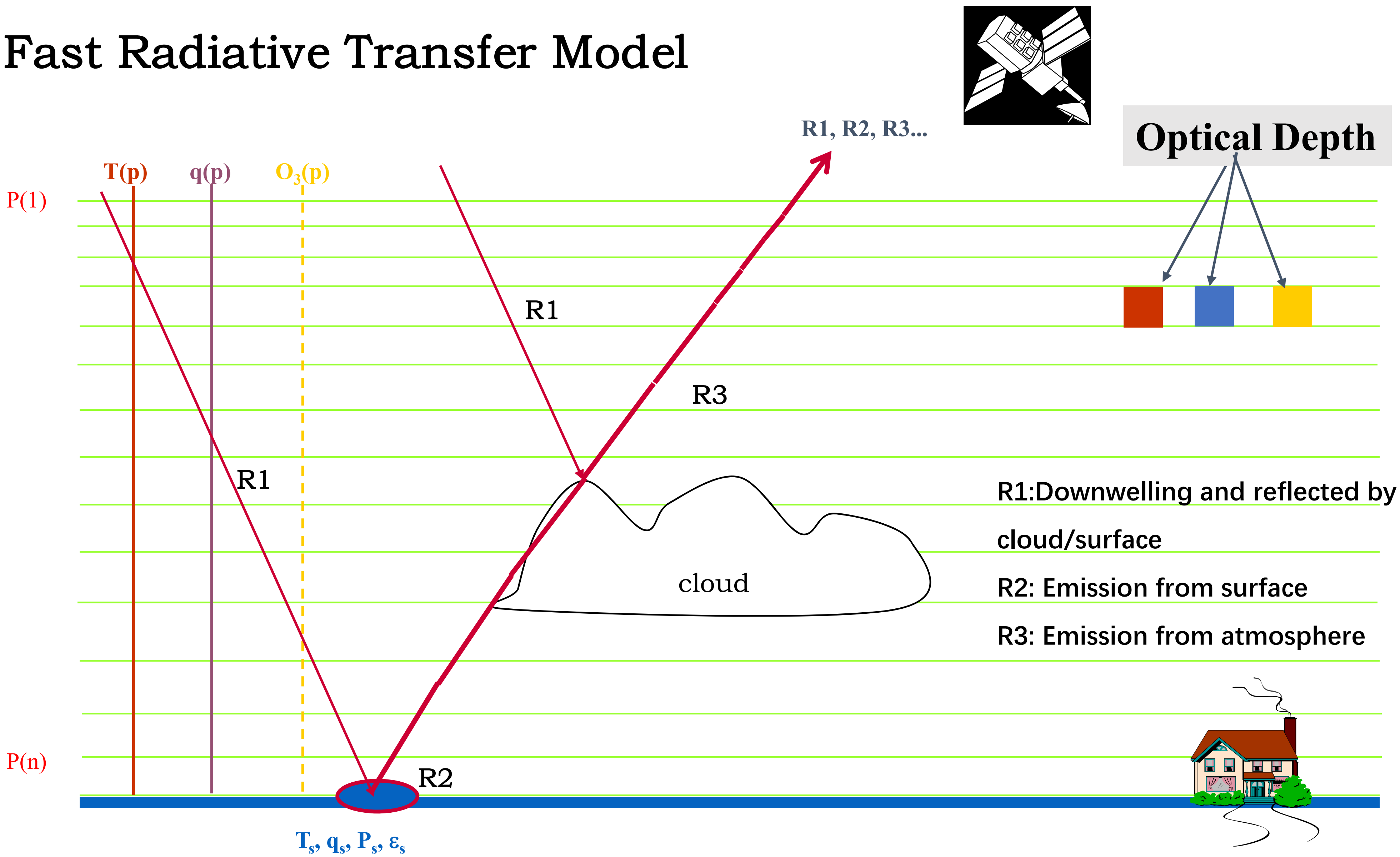

# LBL

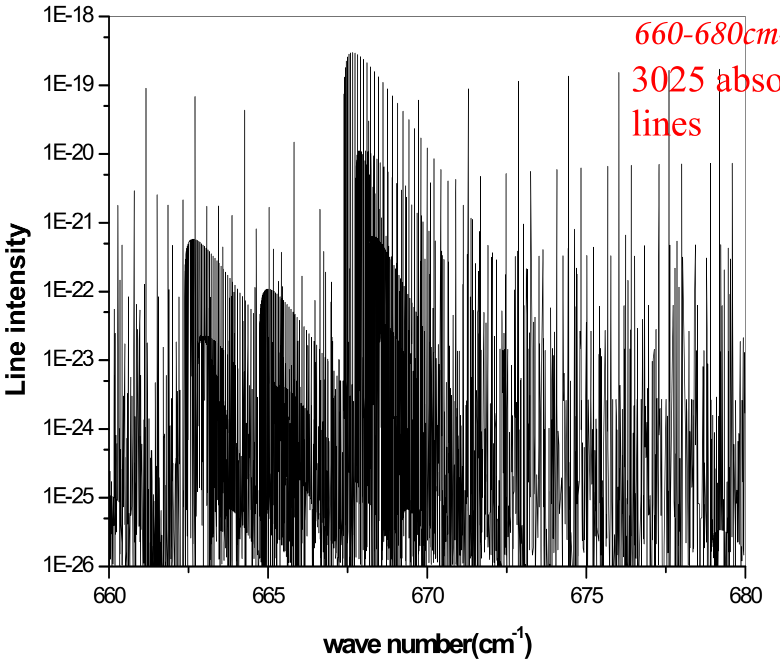


*660-680cm-1*: 3025 absorb lines

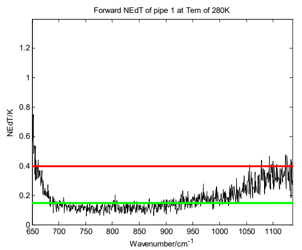


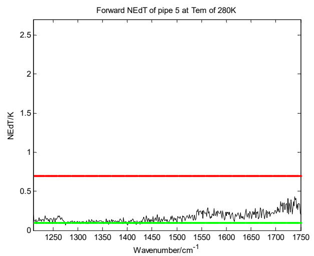


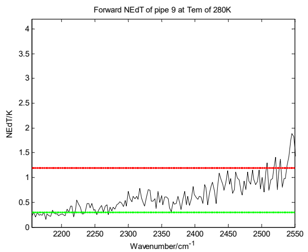


NeδT of HIRAS

2287channels

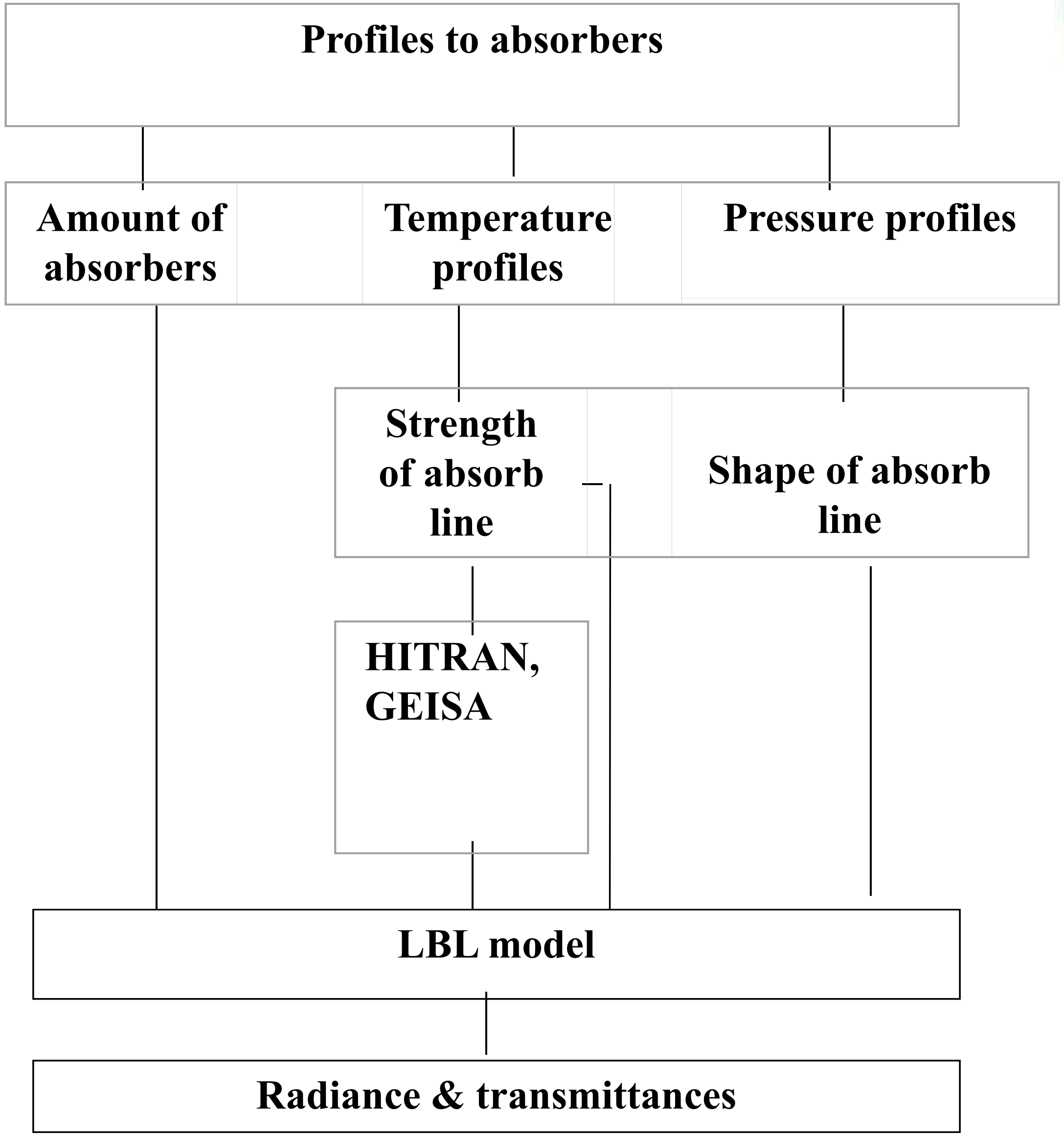

# What is RTTOV

- RTTOV： Radiative Transfer model for TOVS, UK MetOffice, 1993
- TOVS： TIROS Vertical Sounder

$$R_\nu \cong \varepsilon_\nu B_\nu(\Theta_s)T_{s,\nu} + \int_{p_s}^{0} B_\nu(\Theta(p))\frac{\partial T_\nu(p,\theta_u)}{\partial p}dp$$

$$+(1-\varepsilon_\nu)T_{s,\nu}\int_{0}^{p_s} B_\nu(\Theta(p))\frac{\partial T_\nu^*(p,\theta_d)}{\partial p}dp + \rho_\nu T_{s,\nu}T_\nu(p_s,\theta_{sun})F_{0,\nu}\cos\theta_{sun}$$

$$\boxed{d_{i,j} = d_{i,j-1} + \sum_{k=1}^{K} a_{i,j,k} X_{k,j}}$$

d: optical depth to satellite channels

X: predictors to d and depend on atmosphere status

a: coefficients to d and response to spectral characters of channels

# Predictors – RTTOV v7

| Predictor | Fixed gases | Water vapour | Ozone |
|---|---|---|---|
| $X_{j,1}$ | $sec(\theta)$ | $sec^2(\theta) W_r^2(j)$ | $sec(\theta) O_r(j)$ |
| $X_{j,2}$ | $sec^2(\theta)$ | $(sec(\theta) W_w(j))^2$ | $\sqrt{sec(\theta) O_r(j)}$ |
| $X_{j,3}$ | $sec(\theta) T_r(j)$ | $(sec(\theta) W_w(j))^4$ | $sec(\theta) O_r(j) \delta T(j)$ |
| $X_{j,4}$ | $sec(\theta) T_r^2(j)$ | $sec(\theta) W_r(j) \delta T(j)$ | $(sec(\theta) O_r(j))^2$ |
| $X_{j,5}$ | $T_r(j)$ | $\sqrt{sec(\theta) W_r(j)}$ | $\sqrt{sec(\theta) O_r(j)}\ \delta T(j)$ |
| $X_{j,6}$ | $T_r^2(j)$ | $\sqrt[4]{sec(\theta) W_r(j)}$ | $sec(\theta) O_r(j)^2 O_w(j)$ |
| $X_{j,7}$ | $sec(\theta) T_w(j)$ | $sec(\theta) W_r(j)$ | $\frac{O_r(j)}{O_w(j)} \sqrt{sec(\theta) O_r(j)}$ |
| $X_{j,8}$ | $sec(\theta) \frac{T_w(j)}{T_r(j)}$ | $(sec(\theta) W_r(j))^3$ | $sec(\theta) O_r(j) O_w(j)$ |
| $X_{j,9}$ | $\sqrt{sec(\theta)}$ | $(sec(\theta) W_r(j))^4$ | $O_r(j) sec(\theta) \sqrt{(O_w(j) sec(\theta)}$ |
| $X_{j,10}$ | $\sqrt{sec(\theta)}\ \sqrt[4]{T_w(j)}$ | $sec(\theta) W_r(j) \delta T(j) \mid \delta T(j) \mid$ | $sec(\theta) O_w(j)$ |
| $X_{j,11}$ | 0 | $(\sqrt{sec(\theta) W_r(j)}) \delta T(j)$ | $(sec(\theta) O_w(j))^2$ |
| $X_{j,12}$ | 0 | $\frac{(sec(\theta) W_r(j))^2}{W_w}$ | 0 |
| $X_{j,13}$ | 0 | $\frac{\sqrt{(sec(\theta) W_r(j)} W_r(j)}{W_w(j)}$ | 0 |
| $X_{j,14}$ | 0 | $sec(\theta) \frac{W_r^2(j)}{T_r(j)}$ | 0 |
| $X_{j,15}$ | 0 | $sec(\theta) \frac{W_r^2(j)}{T_r^4(j)}$ | 0 |

| Predictor | Water vapour (continuum) | Carbon dioxide (optional) |
|---|---|---|
| $X_{j,1}$ | $\sec(\theta)\frac{W_r^2(j)}{T_r(j)}$ | $\sec(\theta) CO2_r(j)$ |
| $X_{j,2}$ | $\sec(\theta)\frac{W_r^2(j)}{T_r^4(j)}$ | $T_r^2(j)$ |
| $X_{j,3}$ | $\sec(\theta)\frac{W_r(j)}{T_r(j)}$ | $\sec(\theta) T_r(j)$ |
| $X_{j,4}$ | $\sec(\theta)\frac{W_r(j)}{T_r^2(j)}$ | $\sec(\theta) T_r^2(j)$ |
| $X_{j,5}$ | | $T_r(j)$ |
| $X_{j,6}$ | | $\sec(\theta)$ |
| $X_{j,7}$ | | $\sec(\theta) T_{wr}(j)$ |
| $X_{j,8}$ | | $(\sec(\theta) CO2_w(j))^2$ |
| $X_{j,9}$ | | $T_{wr}^3(j)$ |
| $X_{j,10}$ | | $\sec(\theta) T_{wr}(j)\sqrt{T_r}$ |

$$T(j) = [T^{profile}(j) + T^{profile}(j-1)] / 2 \qquad T^*(j) = [T^{reference}(j) + T^{reference}(j-1)] / 2$$

$$W(j) = [W^{profile}(j) + W^{profile}(j-1)] / 2 \qquad W^*(j) = [W^{reference}(j) + W^{reference}(j-1)] / 2$$

$$O(j) = [O^{profile}(j) + O^{profile}(j-1)] / 2 \qquad O^*(j) = [O^{reference}(j) + O^{reference}(j-1)] / 2$$

$$T_r(j) = T(j) / T^*(j) \qquad \delta T(j) = T(j) - T^*(j) \qquad W_r(j) = W(j) / W^*(j)$$

$$O_r(j) = O(j) / O^*(j)$$

$$T_w(j) = \sum_{l=2}^{j} P(l)[P(l) - P(l-1)] T_r(l-1)$$

$$W_w(j) = \left\{\sum_{l=1}^{j} P(l)[P(l) - P(l-1)] W(l)\right\} / \left\{\sum_{l=1}^{j} P(l)[P(l) - P(l-1)] W^*(l)\right\}$$

$$O_w(j) = \left\{\sum_{l=1}^{j} P(l)[P(l) - P(l-1)] O(l)\right\} / \left\{\sum_{l=1}^{j} P(l)[P(l) - P(l-1)] O^*(l)\right\}$$

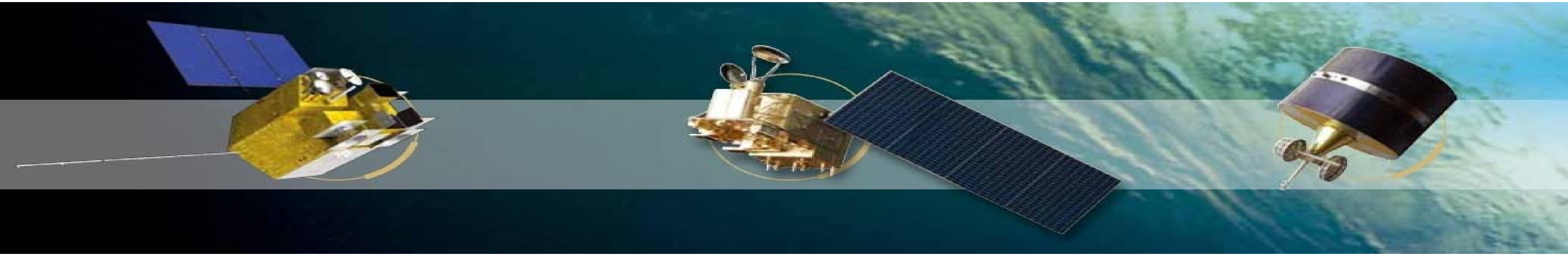

- RTTOV to FY satellite

# RTTOV to FY satellite

Started at Lannion, 1999

- GENLN2， TIGR43，NESDIS34
- RTTOV5
- VIRR of FY1c，VISSR of FY2b

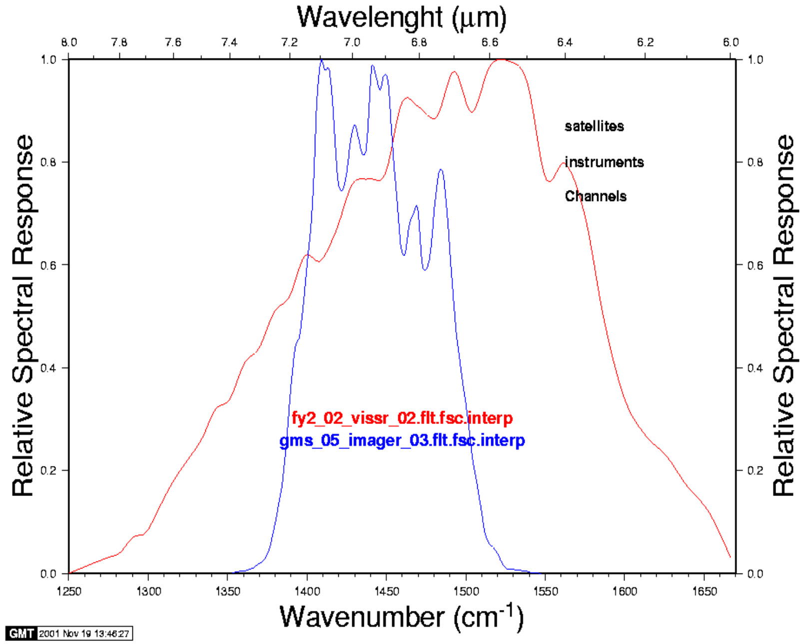


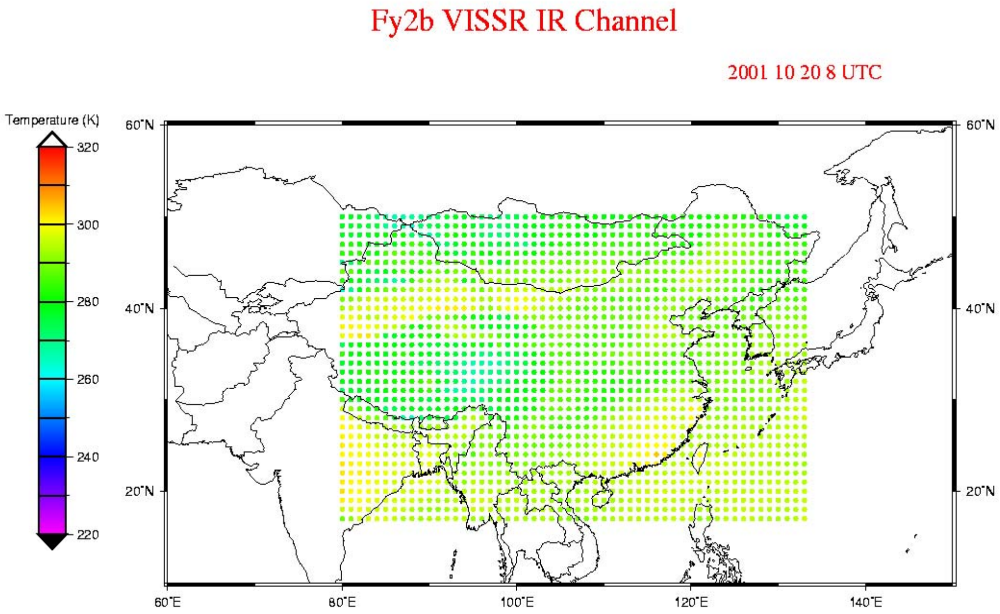

# RTTOV for infrared sensors of FY3

- IRAS 20 infrared channels
- Transmittances data base in 0.5 cm-1 resolution
- Transmittances data base from 600cm-1 – 3000cm-1
- TIGR43 profiles to generate coefficients
- NESDIS34 to do independent test

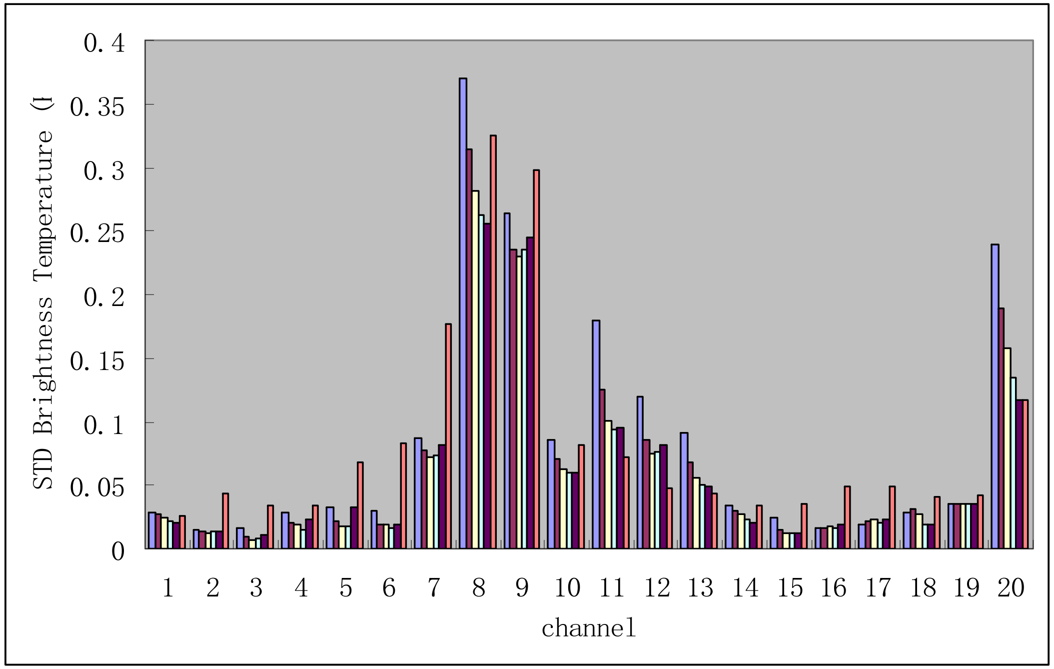

# RTTOV for microwave sensors

- MPM LIEBE89/93
- MONORTM

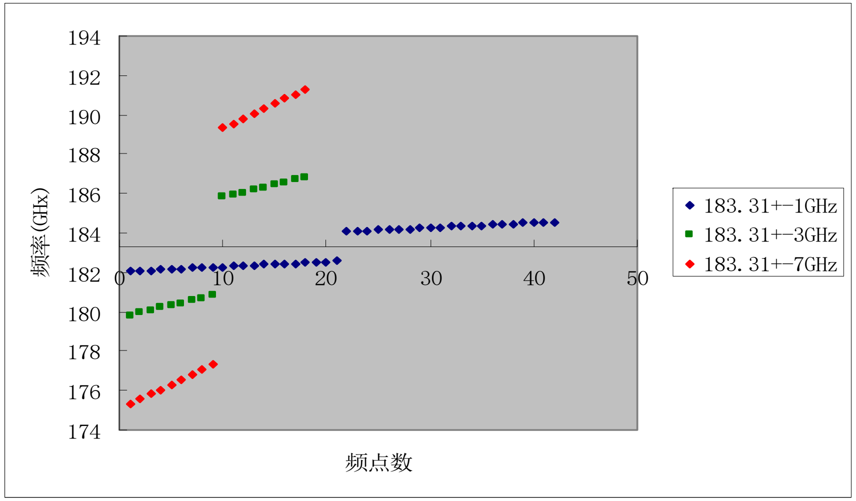


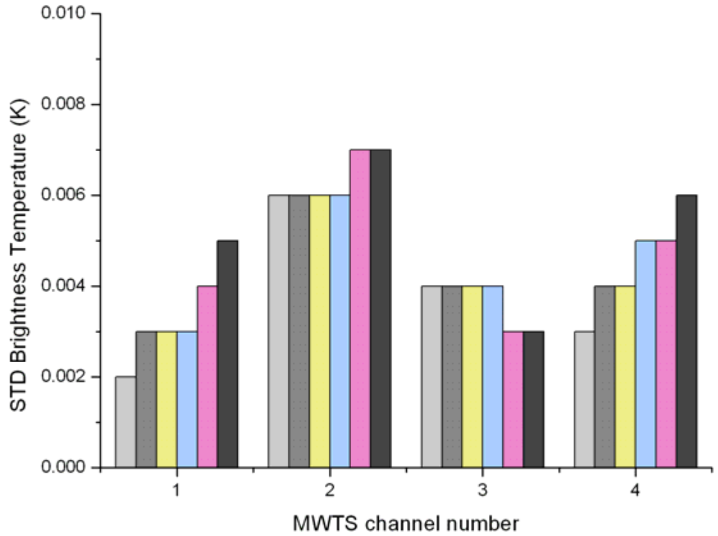


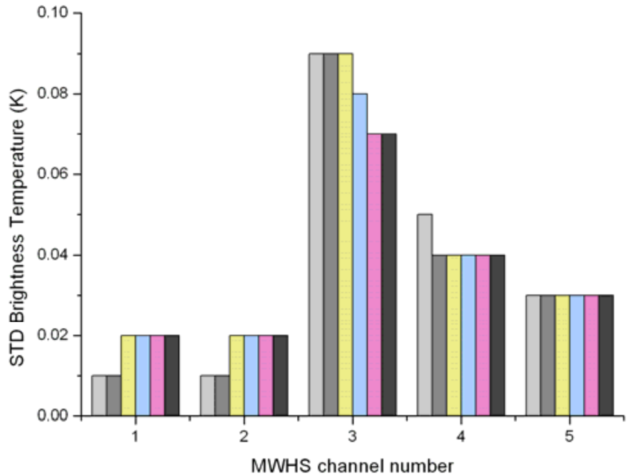

# To improve accuracy of fast model

- Planck weighted convolution to 4.3μm channels

$$\frac{\int F_\nu \cdot L_\nu^{c1r} d\nu}{\int F_\nu d\nu} = \frac{\bar{B}_{T,\nu} \cdot \bar{\varepsilon}_{s,\nu} \cdot \int F_\nu \cdot B_{T,\nu} \cdot \tau_{s,\nu} d\nu}{\int F_\nu \cdot B_{T,\nu} d\nu}$$

$$+ \frac{\bar{B}_{T,\nu} \cdot \int_{\tau_{z,\nu}}^{1} \int F_\nu \cdot B_{T,\nu} d\nu d\tau_\nu}{\int F_\nu \cdot B_{T,\nu} d\nu}$$

$$+ \frac{(1 - \bar{\varepsilon}_{s,\nu}) \cdot \bar{B}_{T,\nu} \cdot \int_{\tau_{z,\nu}}^{1} \int F_\nu \cdot B_{T,\nu} d\nu d\tau_\nu}{\int F_\nu \cdot B_{T,\nu} d\nu}$$

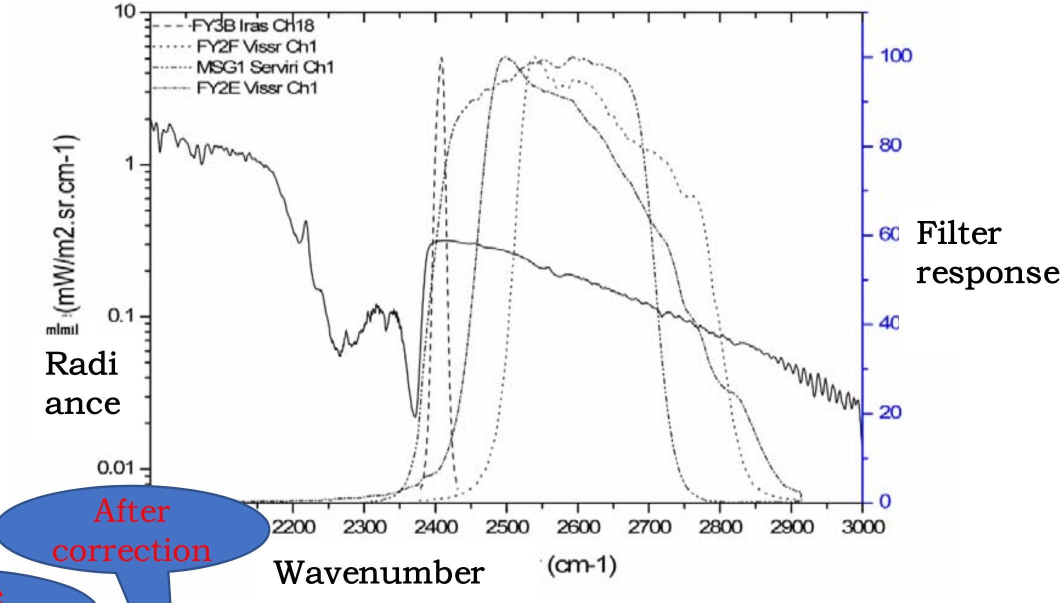


After correction

Before correction

mean

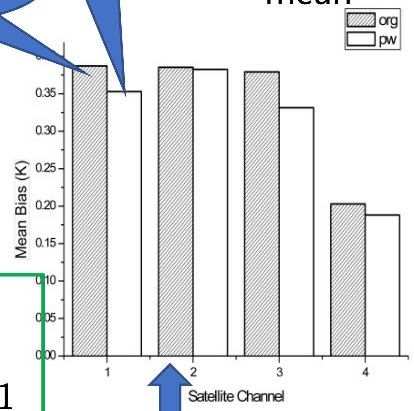


STD

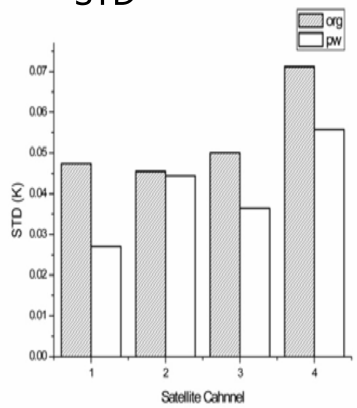


1: VISSR/FY2E
2: VISSR/ FY2F
3: SERVIRI /MSG1
4: IRAS/FY3B

# Analysis to predictors of water line absorption

$\frac{\sqrt{Sec(\theta)W_r^{3}(j)}}{W_{**}(j)}$

$Sec(\theta)W_r(j)\cdot\sqrt{Sec(\theta)W_r(j)}\,\delta T(j)$

## RTTOV v7

Predictors：13

$Sec(\theta)W_r(j)$

$\sqrt{Sec(\theta)W_r(j)}$

$\frac{(Sec(\theta)W_r(j))^2}{W_*(j)}$

$Sec(\theta)W_r(j)\delta T(j)$

$Sec^2(\theta)W_r^{2}(j)$

$(\sqrt{Sec(\theta)W_r(j)})\delta T(j)$

$\sqrt[4]{Sec(\theta)W_r(j)}$

$\frac{(\sqrt{Sec(\theta)W_r(j)})W_r(j)}{W_*(j)}$

$(Sec(\theta)W_r(j))^3$

$(Sec(\theta)W_r(j))^4$

$Sec(\theta)W_r(j)\delta T(j)\left|\delta T(j)\right|$

$(Sec(\theta)W_*(j))^4$

$(Sec(\theta)W_*(j))^2$

## RTTOV v8

Predictors：12

$Sec^2(\theta)W_r^{2}(j)$

$Sec(\theta)W_*(j)$

$Sec(\theta)W_*^{2}(j)$

$Sec(\theta)W_r(j)\delta T(j)$

$\sqrt{Sec(\theta)W_r(j)}$

$\sqrt[4]{Sec(\theta)W_r(j)}$

$Sec(\theta)W_r(j)$

$(Sec(\theta)W_r(j))^3$

$Sec(\theta)W_r(j)\delta T(j)\left|\delta T(j)\right|$

$(\sqrt{Sec(\theta)W_r(j)})\delta T(j)$

$\frac{Sec(\theta)W_r^{2}(j)}{W_{**}(j)}$

$\frac{Sec(\theta)\sqrt{W_r^{3}(j)}}{W_{**}(j)}$

## RTTOV v9

Predictors：19

$Sec^2(\theta)W_r^{2}(j)$

$Sec(\theta)W_*(j)$

$Sec^2(\theta)W_*^{2}(j)$

$Sec(\theta)W_r(j)\delta T(j)$

$\sqrt{Sec(\theta)W_r(j)}$

$\sqrt[4]{Sec(\theta)W_r(j)}$

$Sec(\theta)W_r(j)$

$(Sec(\theta)W_r(j))^3$

$(Sec(\theta)W_r(j))^4$

$Sec(\theta)W_r(j)\delta T(j)\left|\delta T(j)\right|$

$(\sqrt{Sec(\theta)W_r(j)})\delta T(j)$

$\frac{Sec(\theta)W_r^{2}(j)}{W_{**}(j)}$

$\frac{Sec(\theta)\sqrt{W_r^{3}(j)}}{W_{**}(j)}$

$Sec(\theta)\sqrt{W_{**}^{3}(j)}$

$Sec(\theta)\sqrt{W_r^{3}(j)}$

$\frac{Sec(\theta)W_{**}(j)\sqrt[4]{W_{**}(j)}}{\sqrt{Sec(\theta)W_r(j)}\cdot W_r(j)}$

## CRTM 2.1

Predictors：14

$Sec(\theta)W_r(j)$

$Sec(\theta)W_r(j)\delta T(j)$

$Sec^2(\theta)W_r^{2}(j)$

$Sec(\theta)W_r(j)\delta T(j)\left|\delta T(j)\right|$

$\sqrt[4]{Sec(\theta)W_r(j)}$

$(Sec(\theta)W_r(j))^3$

$\sqrt{Sec(\theta)W_r(j)}$

$(\sqrt{Sec(\theta)W_r(j)})\delta T(j)$

$(Sec(\theta)W_r(j))^4$

$\frac{Sec(\theta)W_r(j)}{W_{**}(j)}$

$\frac{Sec(\theta)\sqrt{W_r^{3}(j)}}{W_{**}(j)}$

$Sec^2(\theta)W_*^{2}(j)$

$Sec(\theta)W_*(j)$

$Sec(\theta)$

# Coefficients of AGRI to various optical depth predictor

LBL：GENLN2（Mixed gas，Water-line，Ozone），CKD2.1（Water Continum）
Profile Data：NESDIS 34
Layers：43,1013.25-0.1hPa

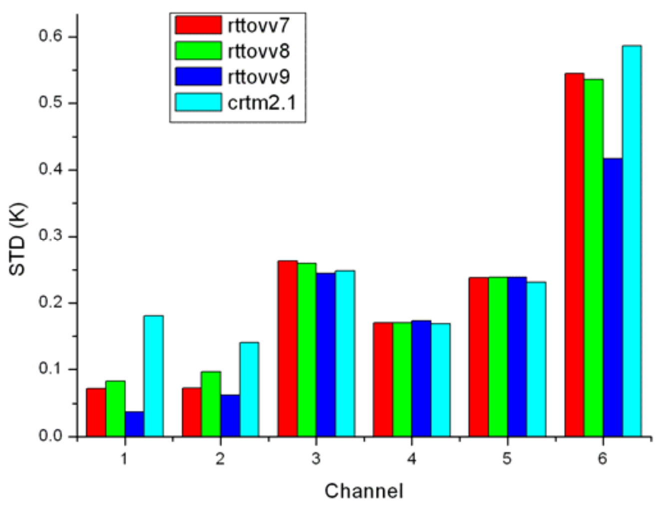


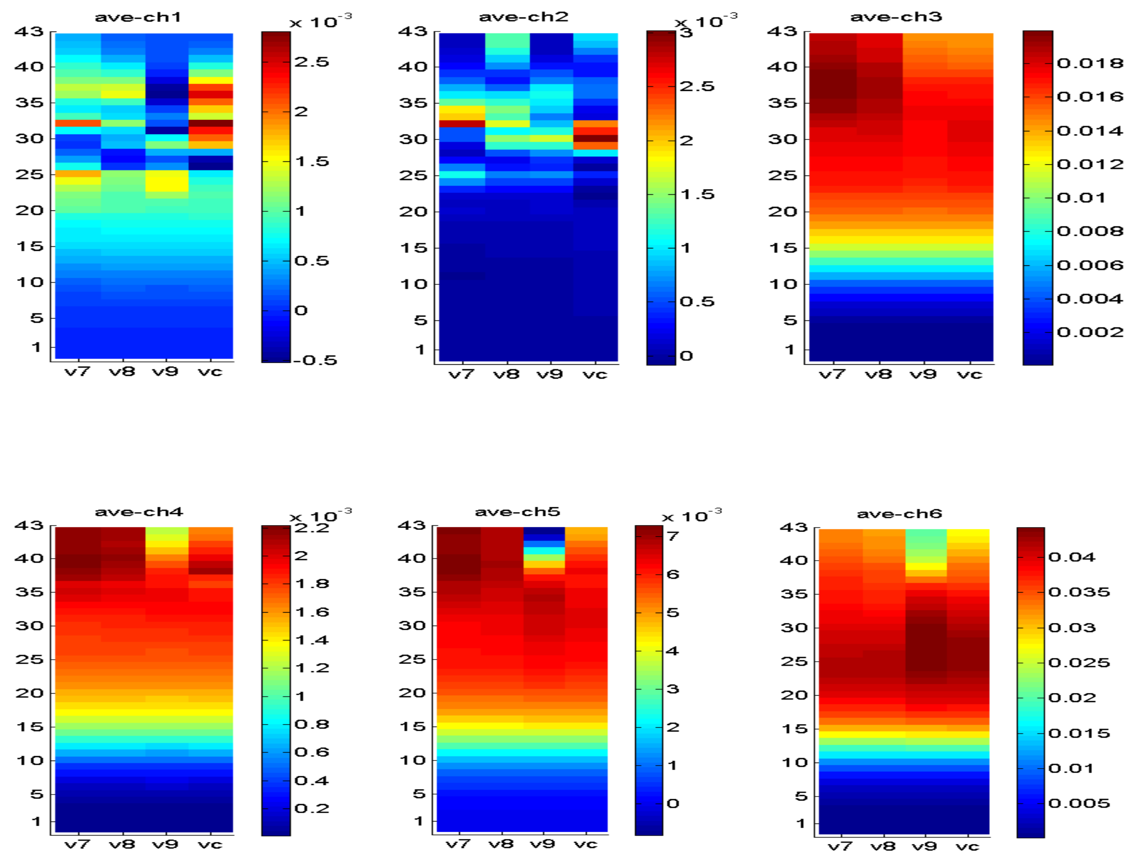

# Profiles database

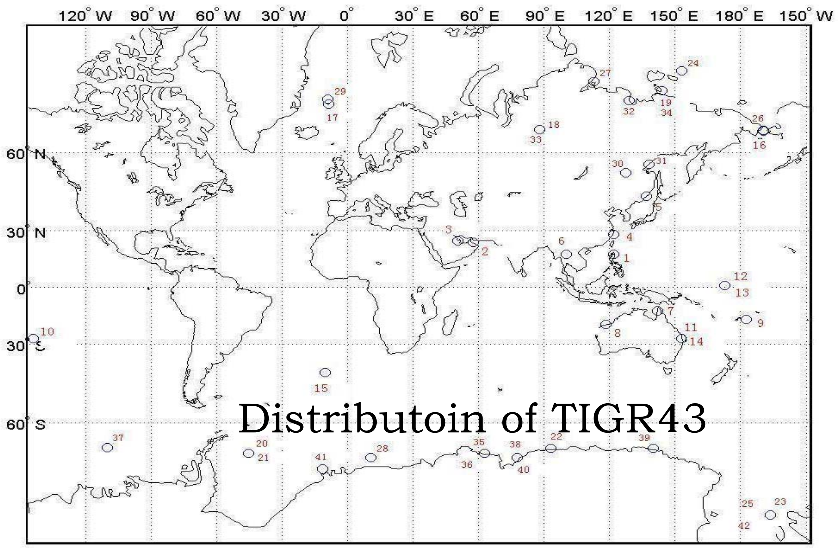


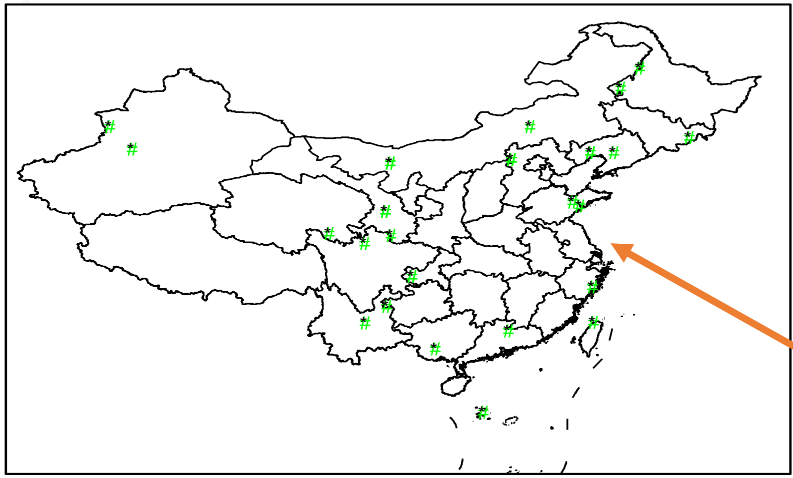

30 typical profiles in China

| ID of layer | Type 1 (hPa) | Type 2 (hPa) | Type 3 (hPa) | Type 4 (hPa) | Type 5 (hPa |
|---|---|---|---|---|---|
| 1 | 20 | 20 | 20 | 20 | 20 |
| 2 | 30 | 30 | 30 | 30 | 30 |
| 3 | 50 | 50 | 50 | 50 | 50 |
| 4 | 70 | 70 | 70 | 70 | 70 |
| 5 | 100 | 100 | 100 | 100 | 100 |
| 6 | 150 | 150 | 150 | 150 | 150 |
| 7 | 200 | 200 | 200 | 200 | 200 |
| 8 | 250 | 250 | 250 | 250 | 250 |
| 9 | 300 | 300 | 300 | 300 | 300 |
| 10 | 400 | 400 | 400 | 400 | 400 |
| 11 | 500 | 500 | 500 | 500 | 500 |
| 12 | | 700 | 700 | 700 | 700 |
| 13 | Tibetan | | 850 | 850 | 850 |
| 14 | | | Loess | 925 | 925 |
| 15 | | | plateau | | 1000 |

Traditional plain

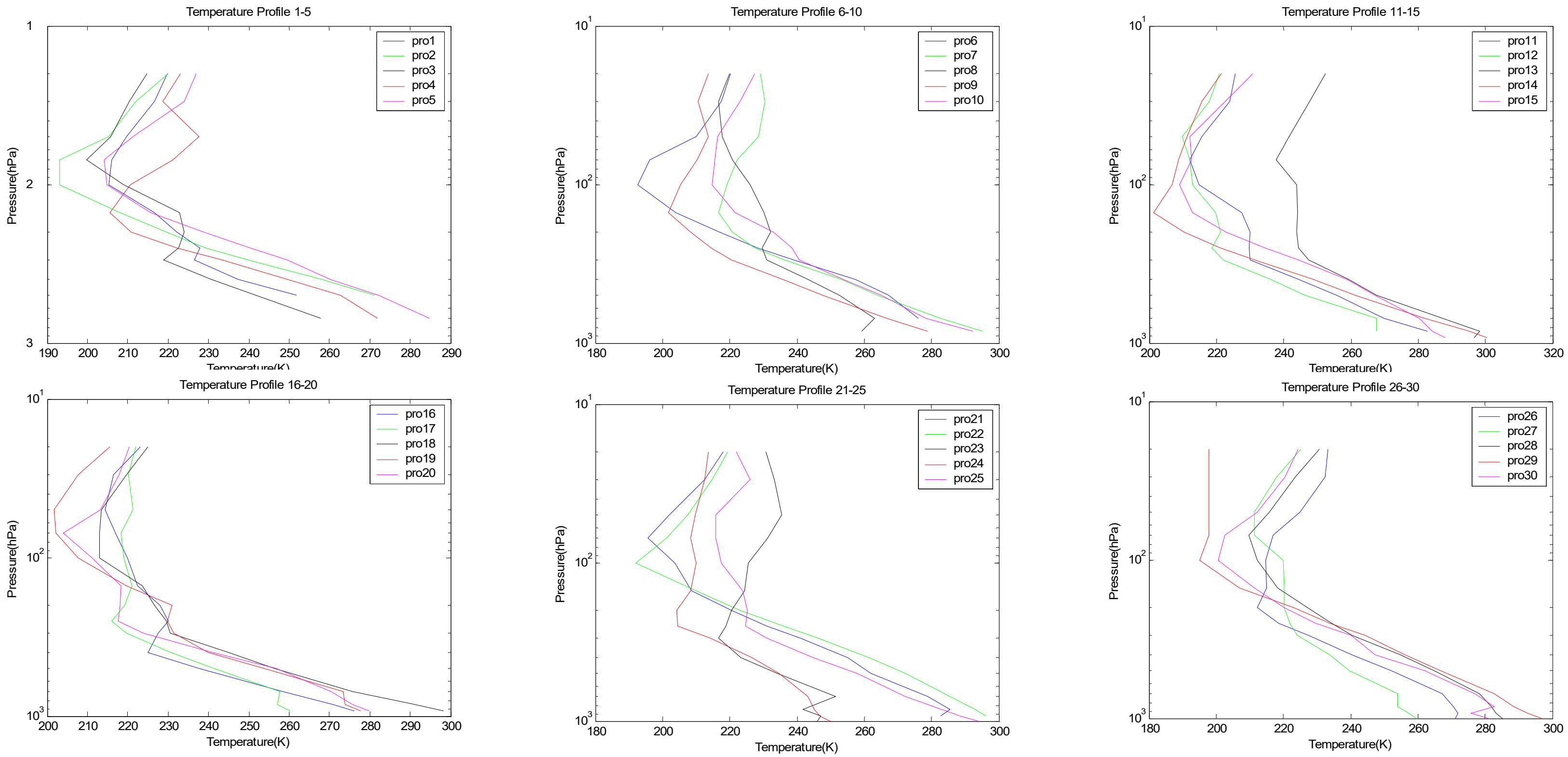


# Temperature gap to typical profiles in China

- **Gap to troposphere top**
- **Gap to temperature at same pressure level**
- **Gap to temperature inversion layer**

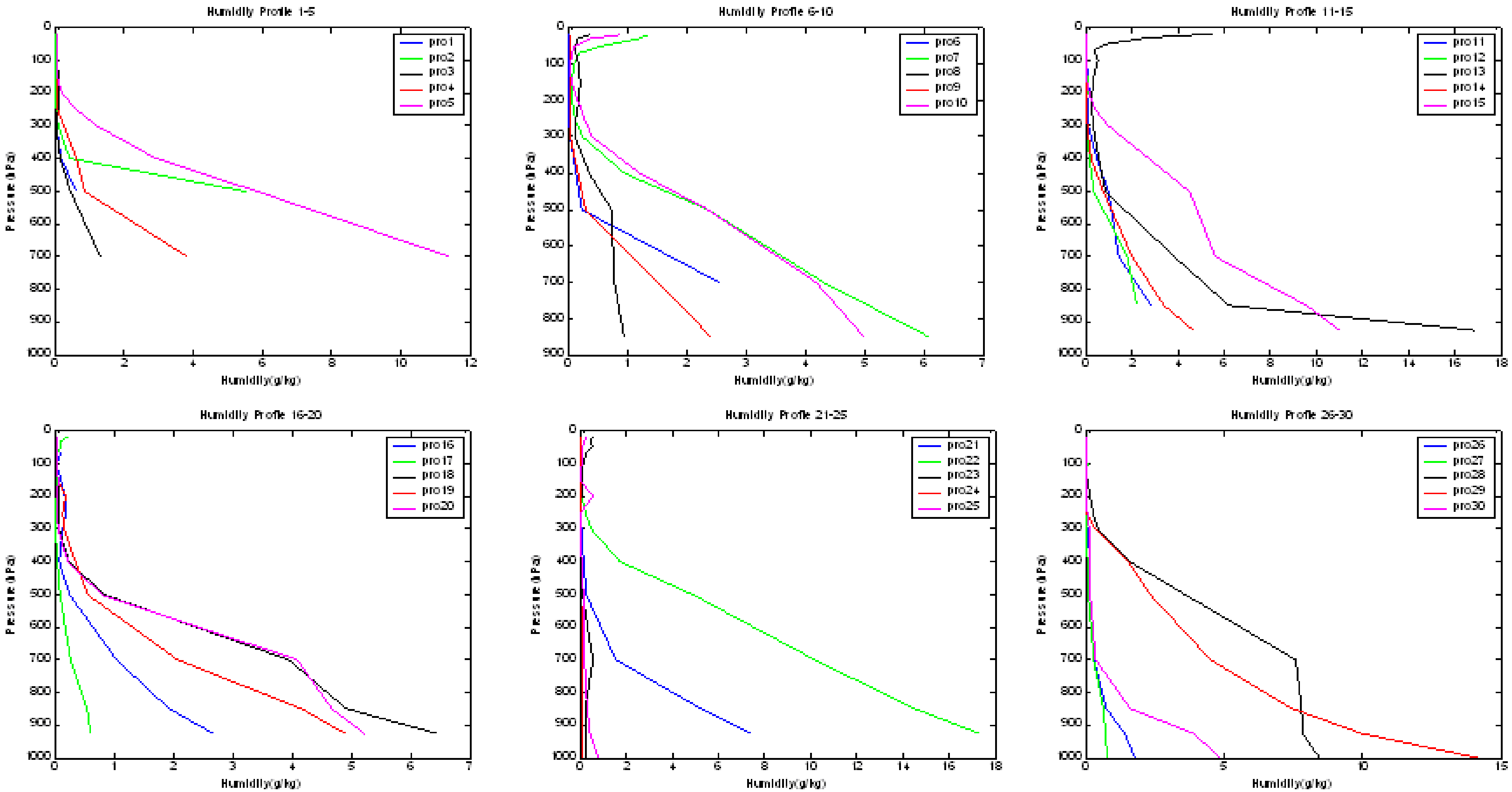


Humidity gap to typical profiles in China

# Transmittances data base (GENLN2 vs LBLRTM)

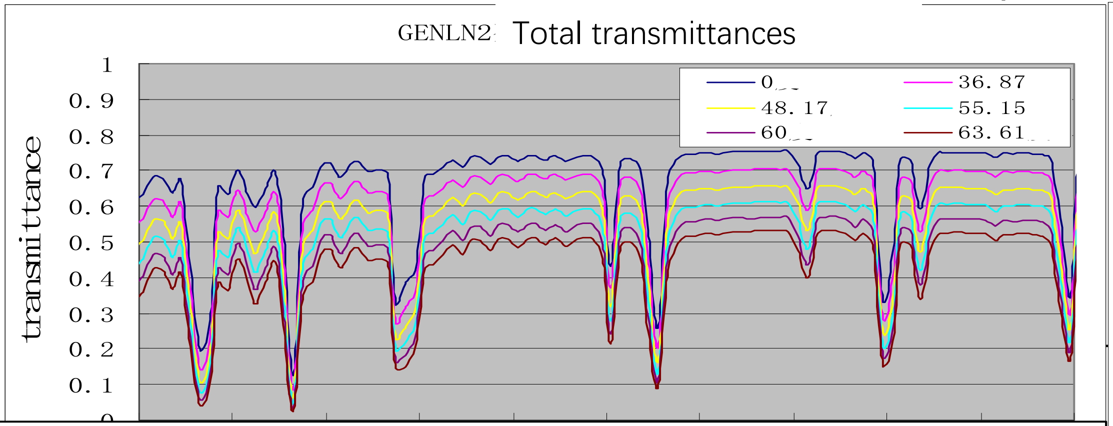


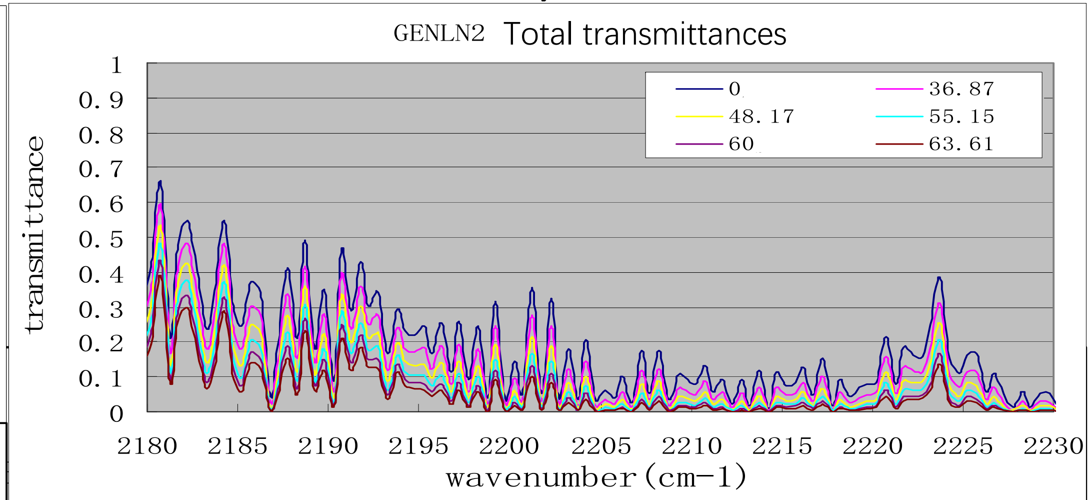


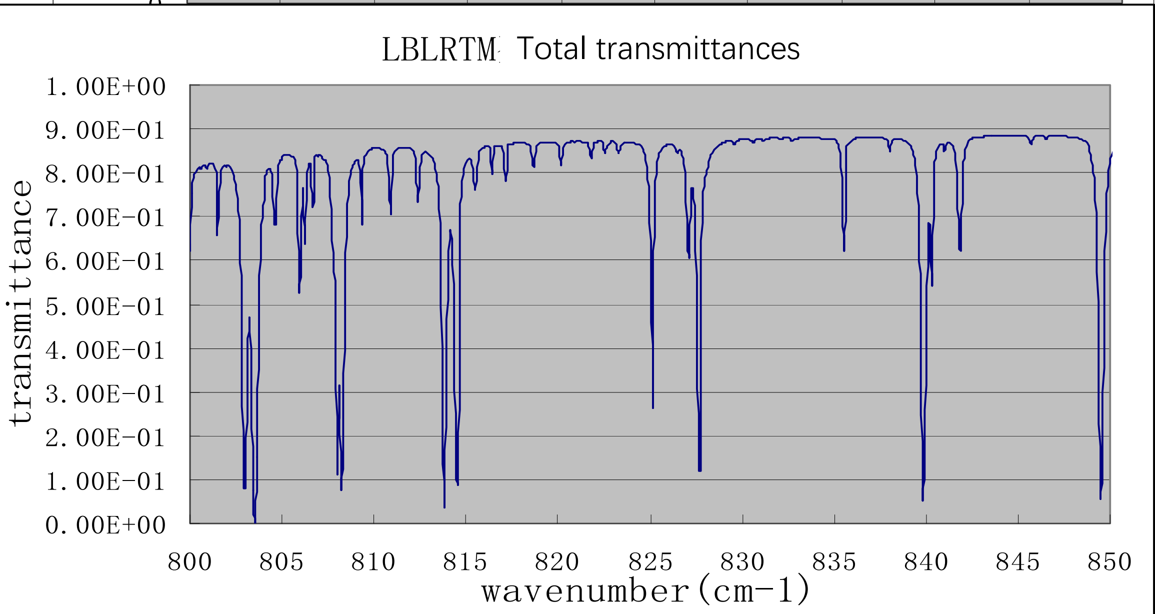


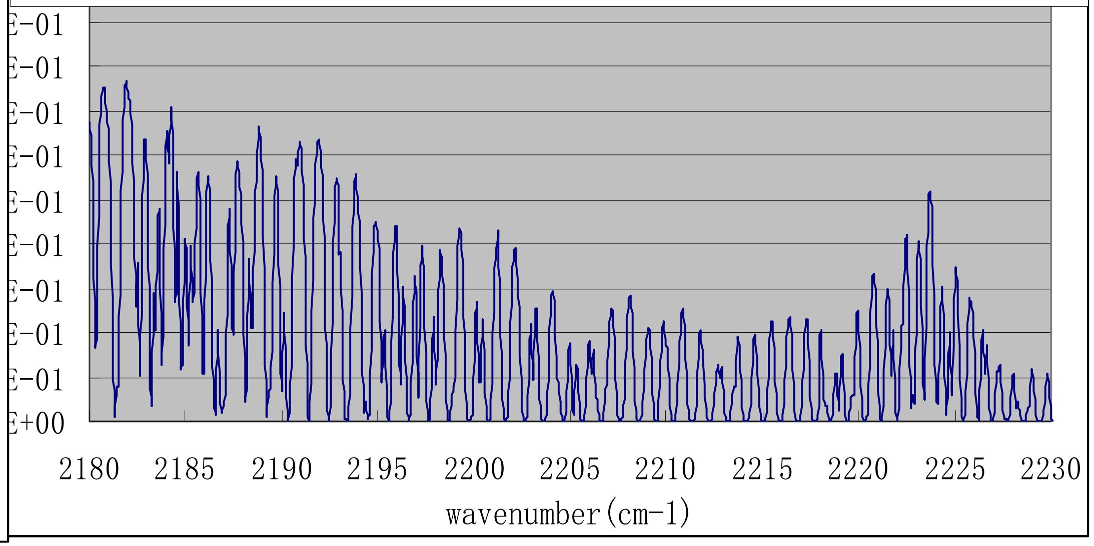

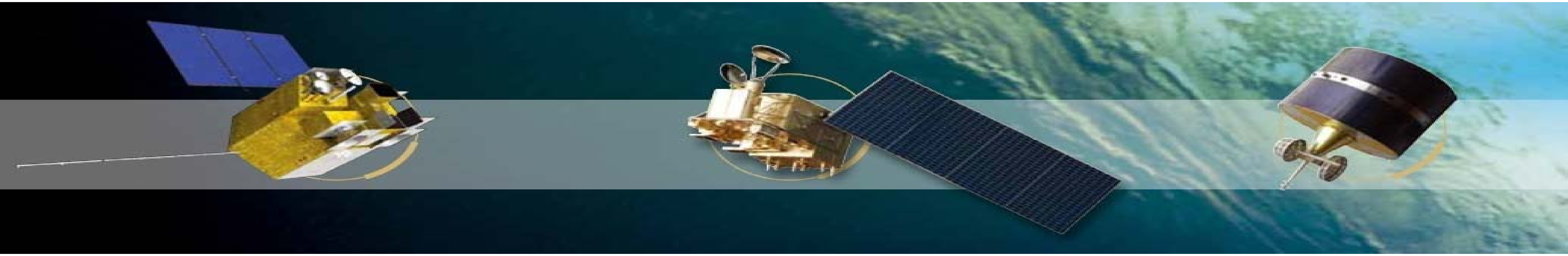

- Pre-Quality Control to assimilation of FY Data

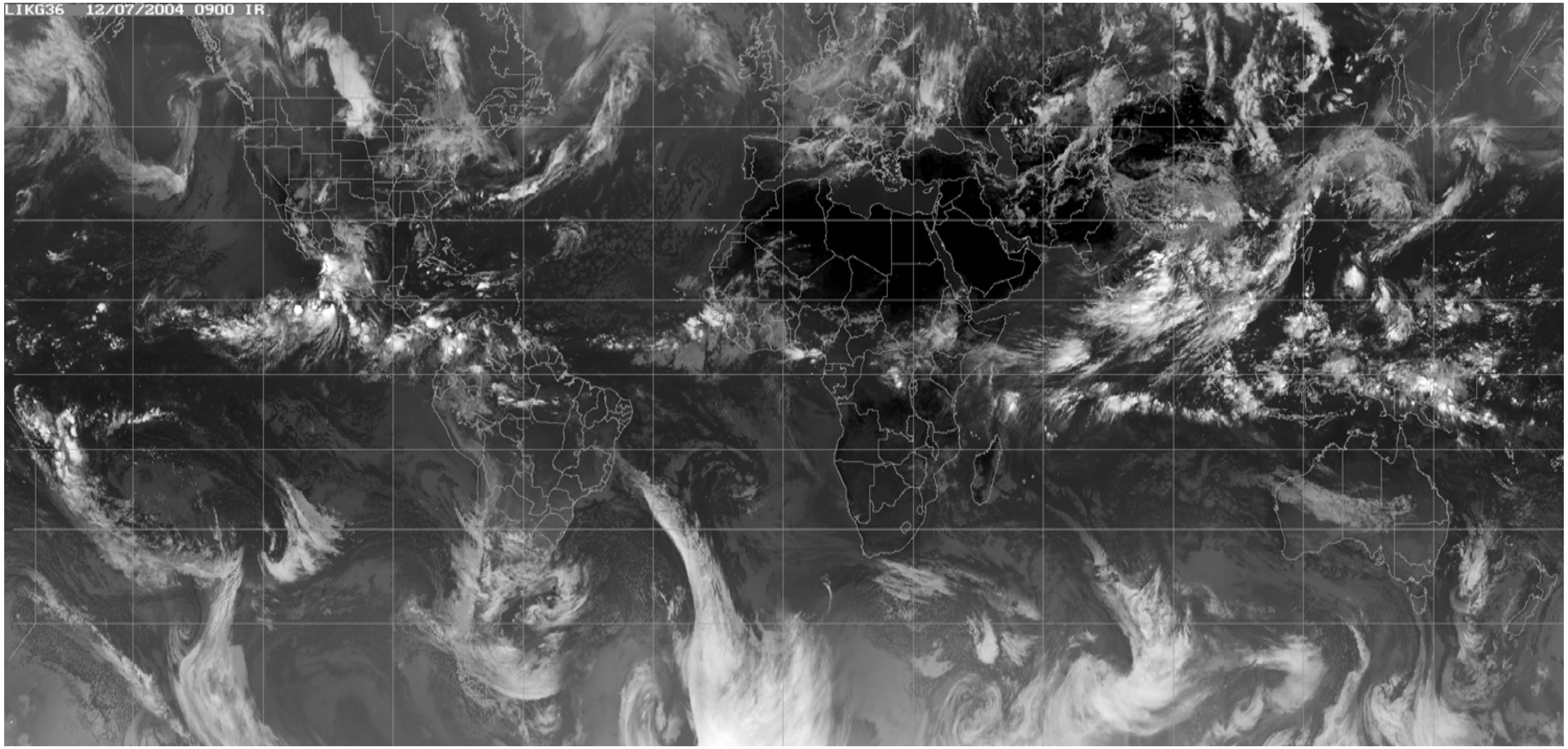


## Cloud is common

| Instrument | Cloud-free | Cloud-free upper-trop |
|---|---|---|
| AIRS (14 km) | 5% | 30% |
| AMSU (50 km) | 70% | 95% |

# 微波波段温度探测仪器

## AMSU-A

| ID | Cnetral frequency (GHz) | absorber |
|---|---|---|
| 1 | 23.8 | $H_2O$ |
| 2 | 31.4 | Window |
| 3 | 50.3 | Window |
| 4 | 52.8 | $O_2$ |
| 5 | 53.596+/−0.115 | $O_2$ |
| 6 | 54.4 | $O_2$ |
| 7 | 54.94 | $O_2$ |
| 8 | 55.5 | $O_2$ |
| 9 | $f_0$=57.29±0.344 | $O_2$ |
| 10 | $f_0$±0.217 | $O_2$ |
| 11 | $f_0$±0.3222±0.048 | $O_2$ |
| 12 | $f_0$±0.3222±0.022 | $O_2$ |
| 13 | $f_0$±0.3222±0.010 | $O_2$ |
| 14 | $f_0$±0.3222±0.045 | $O_2$ |
| 15 | 89.0 | Window |

## MWTS

| ID | Central frequency(GHz) | absorbers |
|---|---|---|
| 1 | 50.3 | Window |
| 2 | 53.596±0.115 | $O_2$ |
| 3 | 54.94 | $O_2$ |
| 4 | 57.290 | $O_2$ |

## MWTS II

| ID | Central frequency (GHz) | 3dBband width (MHz) | Use |
|---|---|---|---|
| 1 | 50.3 | 180 | Emissivity |
| 2 | 51.76 | 400 | Sounding to atmospheric temperature |
| 3 | 52.8 | 400 | |
| 4 | 53.596 | 400 | |
| 5 | 54.40 | 400 | |
| 6 | 54.94 | 400 | |
| 7 | 55.50 | 330 | |
| 8 | 57.290344(fo) | 330 | |
| 9 | fo±0.217 | 78 | |
| 10 | fo±0.3222±0.048 | 36 | |
| 11 | fo±0.3222±0.022 | 16 | |
| 12 | fo±0.3222±0.010 | 8 | |
| 13 | fo±0.3222±0.0045 | 3 | |

# Pre-Quality Control to assimilation of FY Data

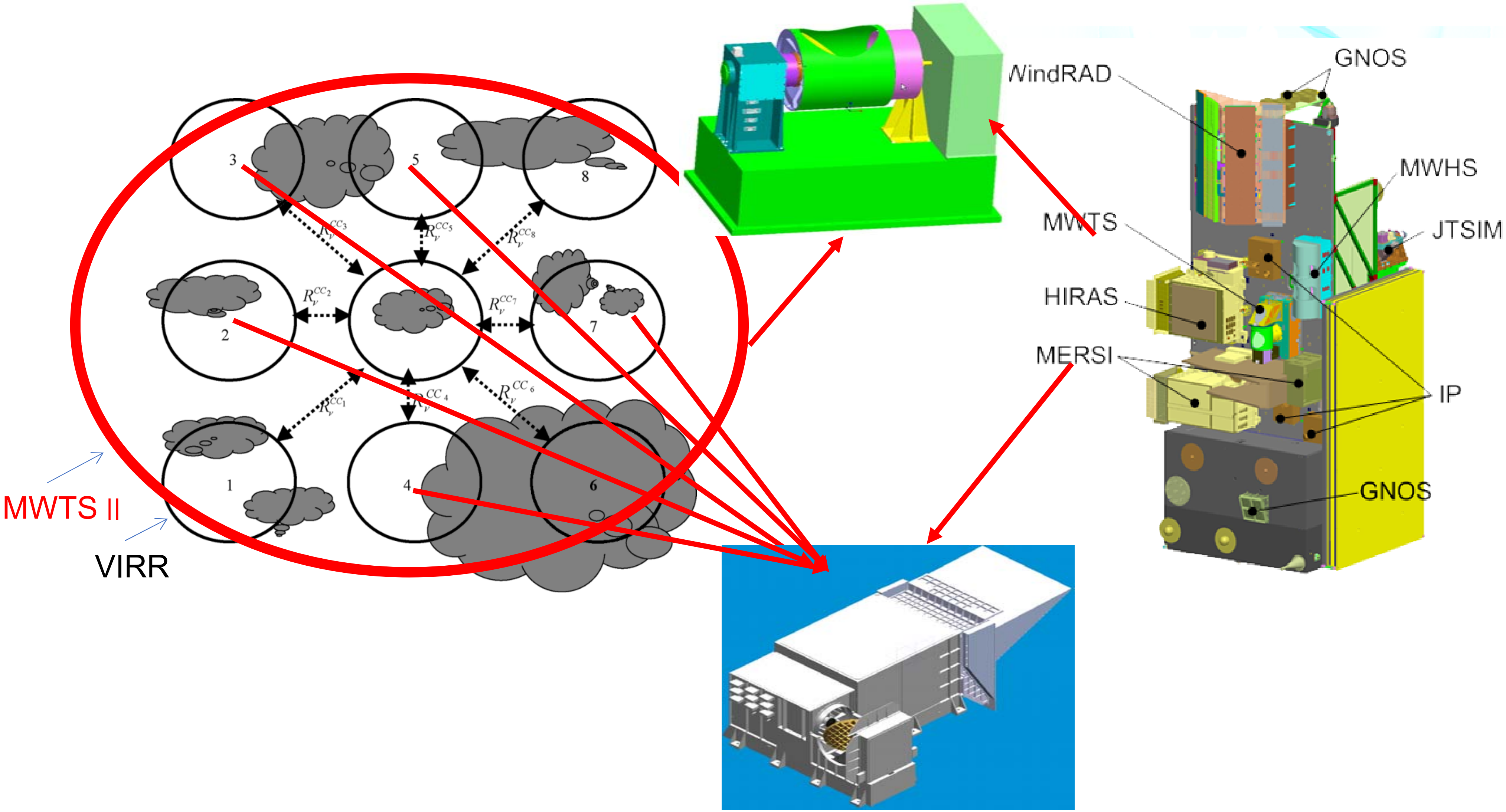

# Pre-Quality Control to assimilation of FY Data

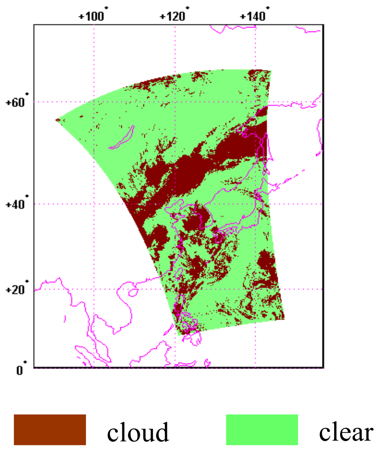


Cloud mask by VIRR

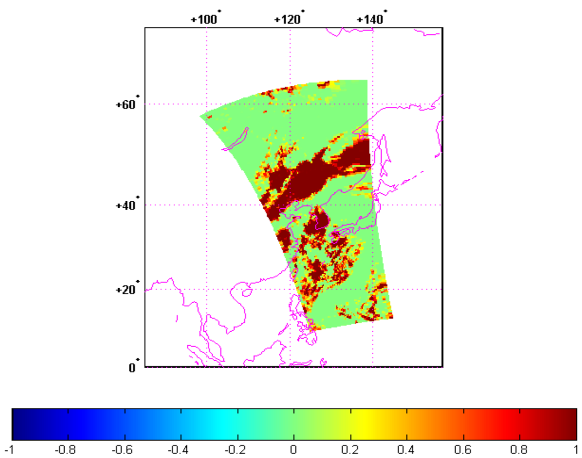


Cloud fraction after matched onto foot-point of MWTS

$$L_i = (1 - N) \cdot L_i^{clr} + N \cdot L_i^{cld}$$

N: cloud fraction
L: radiance in a foot-point

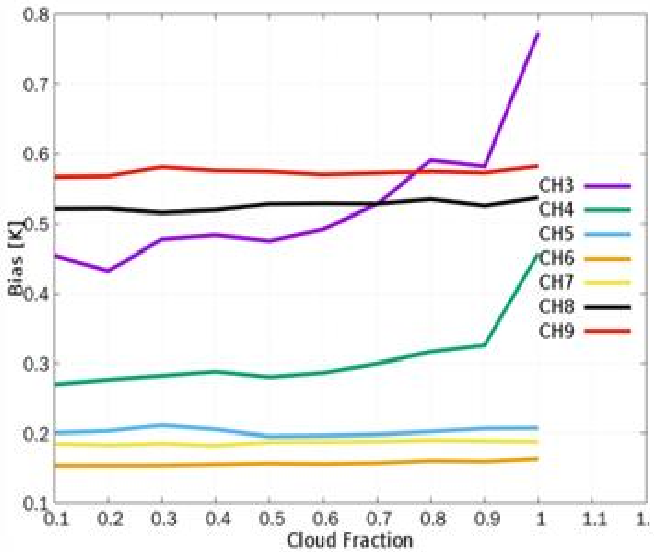


Sensitivity between radiance and cloud fraction

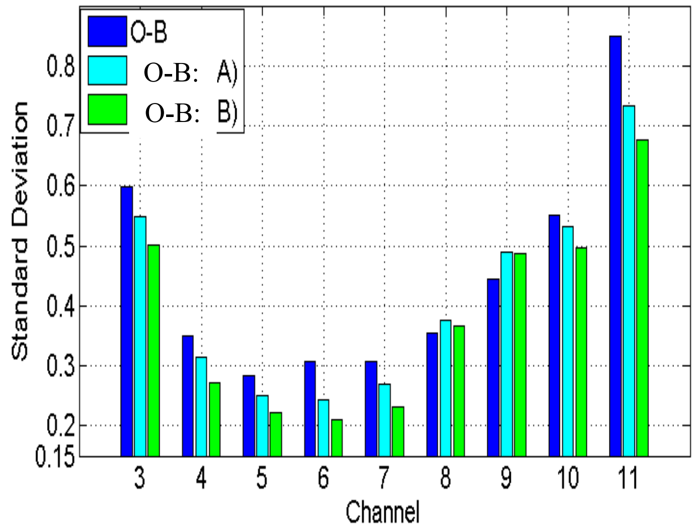


O-B to MWTSII of FY3C

A: QC with O-B only
B: QC with both O-B and cloud fraction

# Pre-Quality Control to assimilation of FY Data

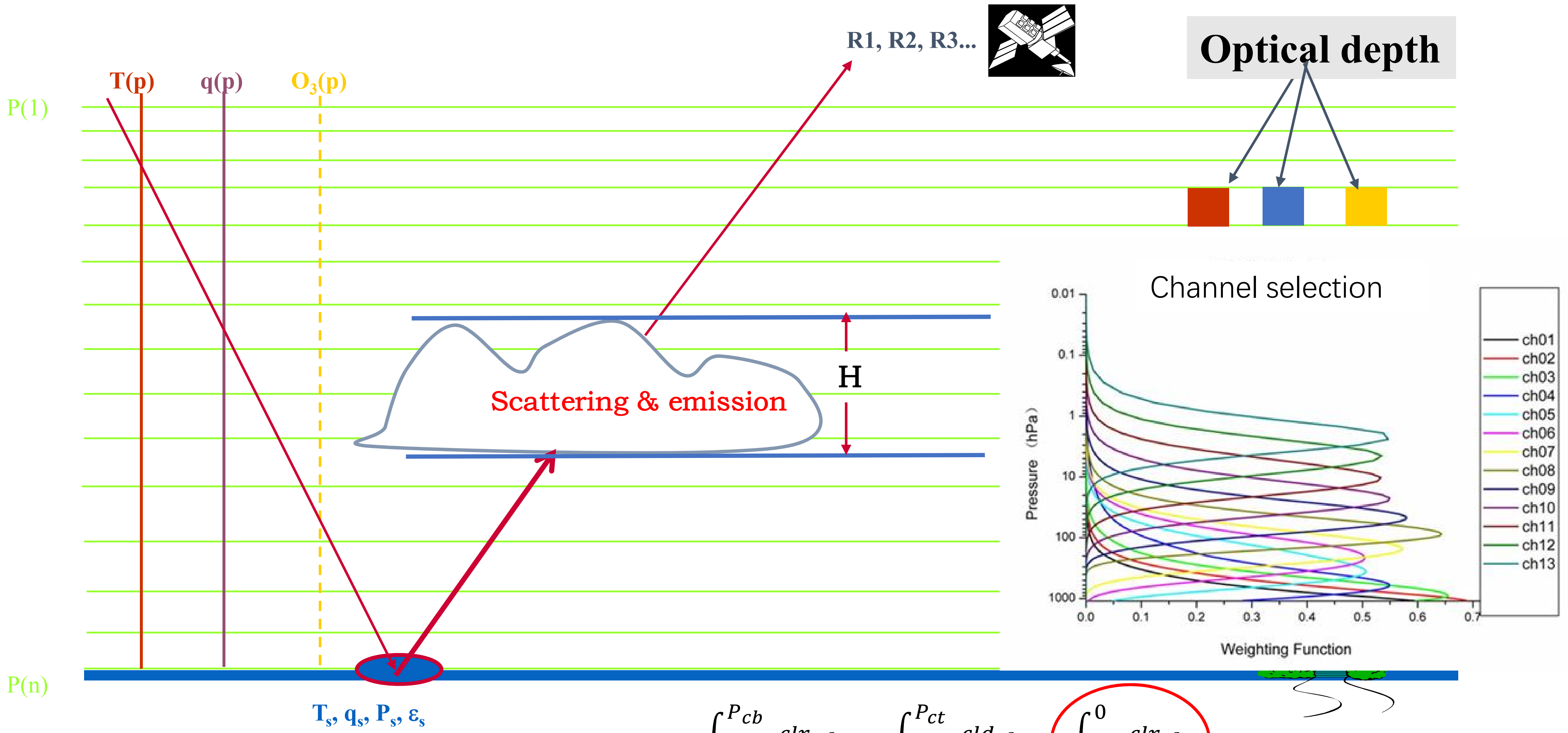


$$L_i = \int_{P_s}^{P_{cb}} L_i^{clr}\, dp + \int_{P_{cb}}^{P_{ct}} L_i^{cld}\, dp + \int_{P_{ct}}^{0} L_i^{clr}\, dp$$

# Multi-layers fast forward model in RTTOV

Radiance to cloudy/partly cloudy pixel

$$L_i = (1 - N_{\max}) \cdot L_i^{clr} + \sum_{j=1}^{k} N_j \cdot L_i^{cld}$$

Efficient cloud fraction at each layer

Maximum cloud fractions at each layer

Radiance to multi-layer cloud

$$L_i^{cld} = \varepsilon_i^{cld} \cdot \tau_{top,i}^{cld} \cdot B(T_{top}^{cld})_i + \int_{P_s}^{P_{top}^{cld}} B(T)_i \cdot \frac{\partial \tau}{\partial P} \cdot dp + (1 - \varepsilon_i^{cld}) \cdot (\tau_{top,i}^{cld})^2 \cdot \int_{P_s}^{P_{top}^{cld}} \frac{B(T)_i}{\tau^2} \cdot \frac{\partial \tau}{\partial P} \cdot dp$$

Clear radiance above cloud top

Reflection at cloud top

# Pre-Quality Control to assimilation of FY Data

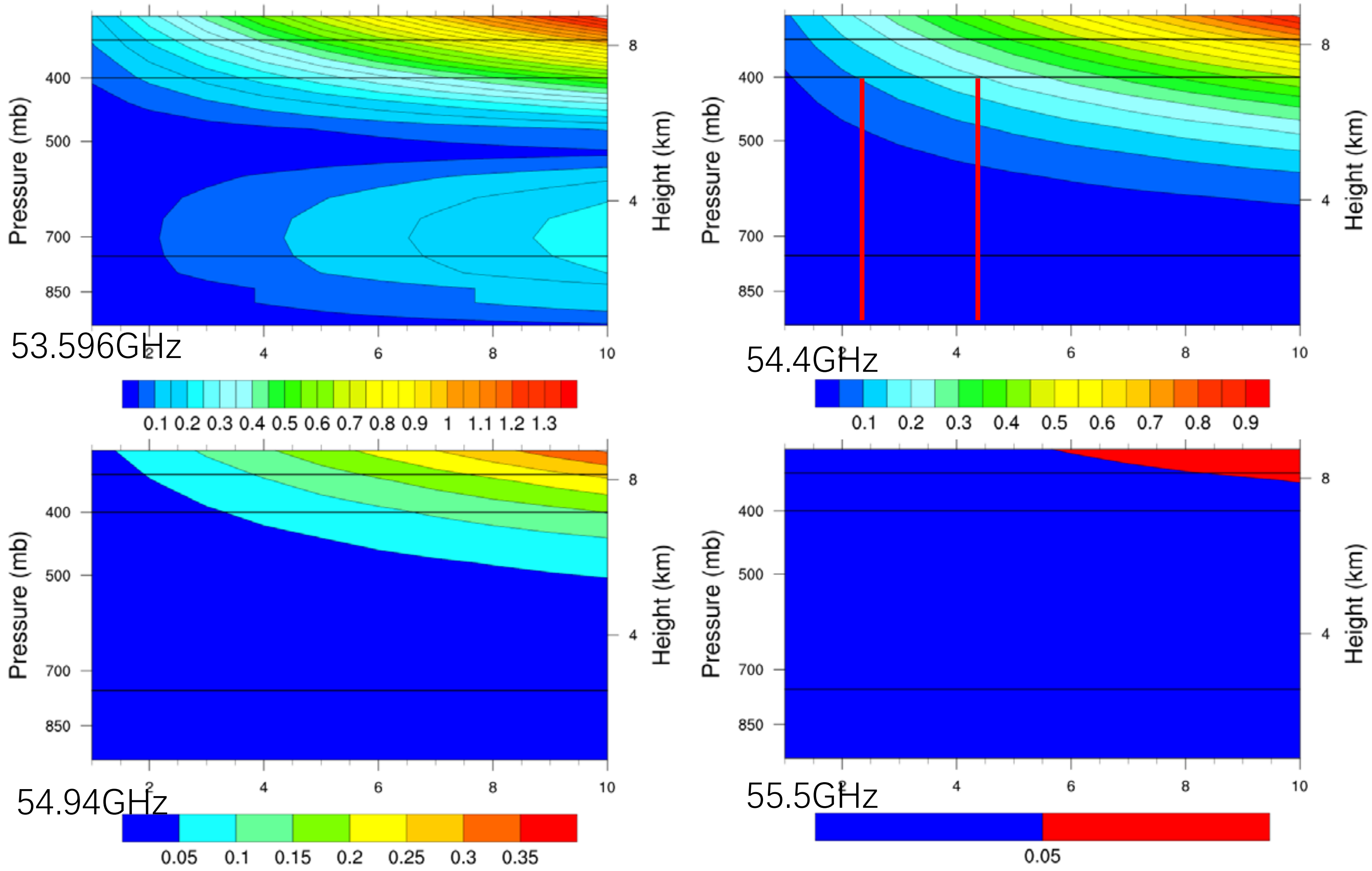

# Pre-Quality Control to assimilation of FY Data

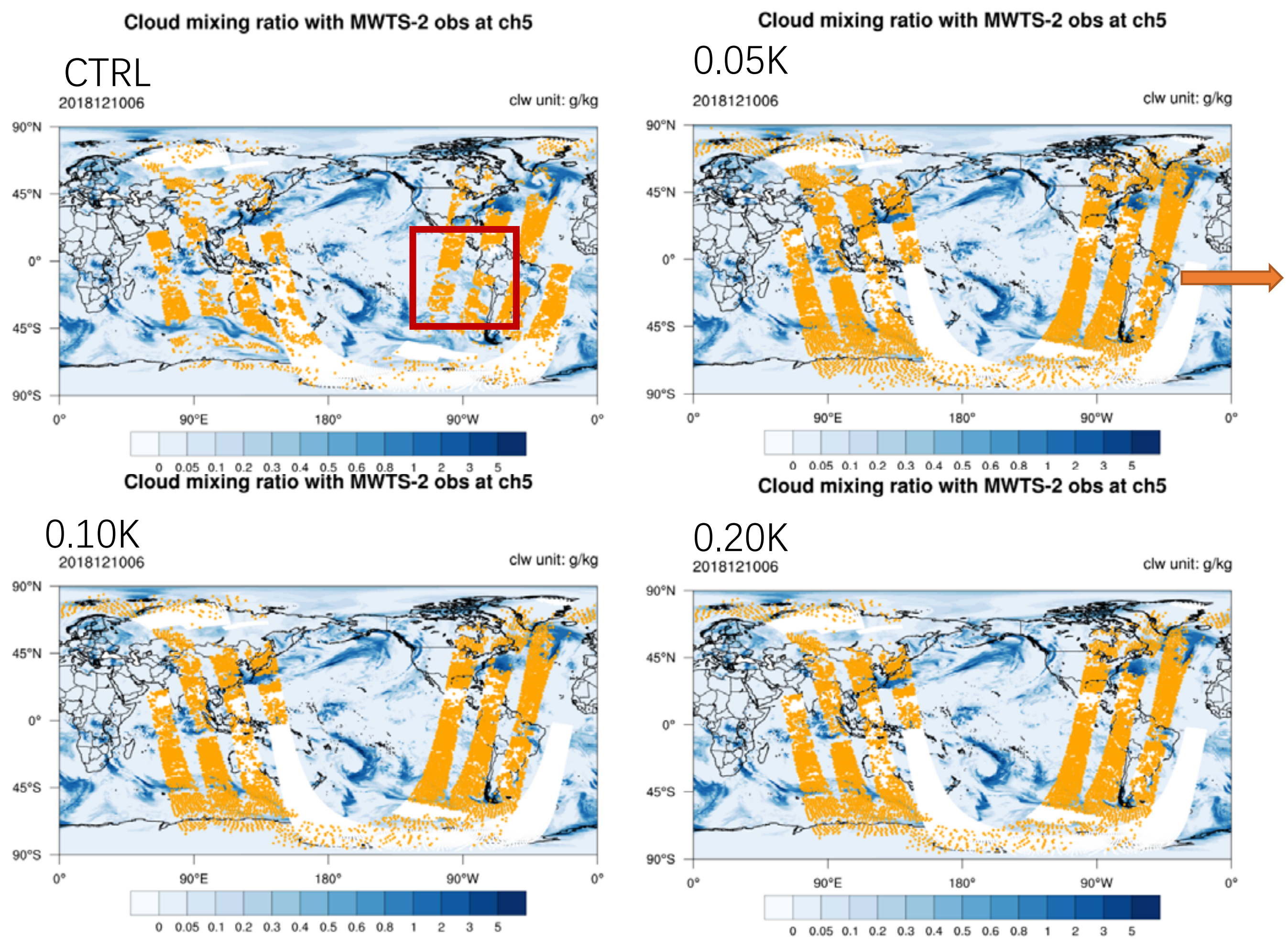

# Pre-Quality Control to assimilation of FY Data

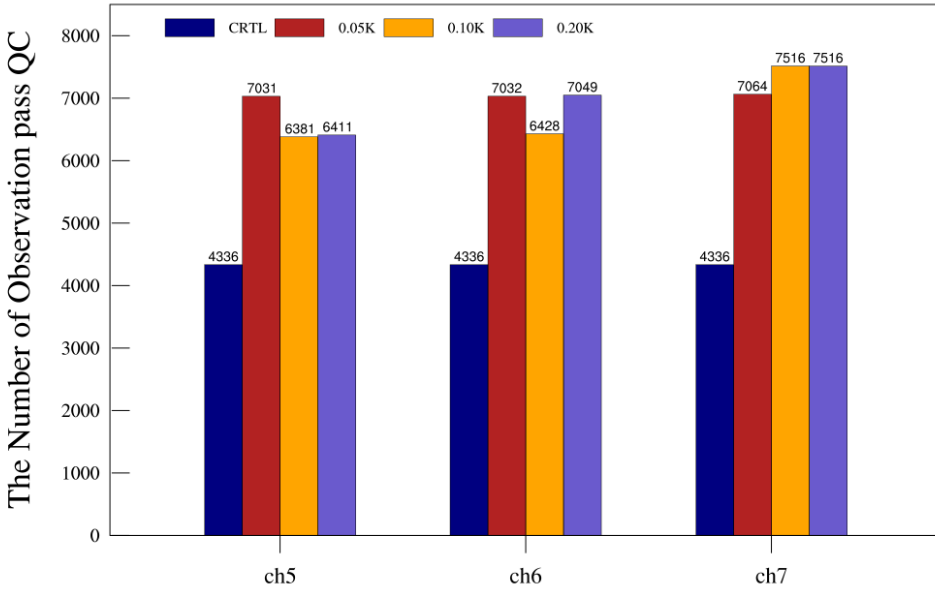


Data used in 3 experiments

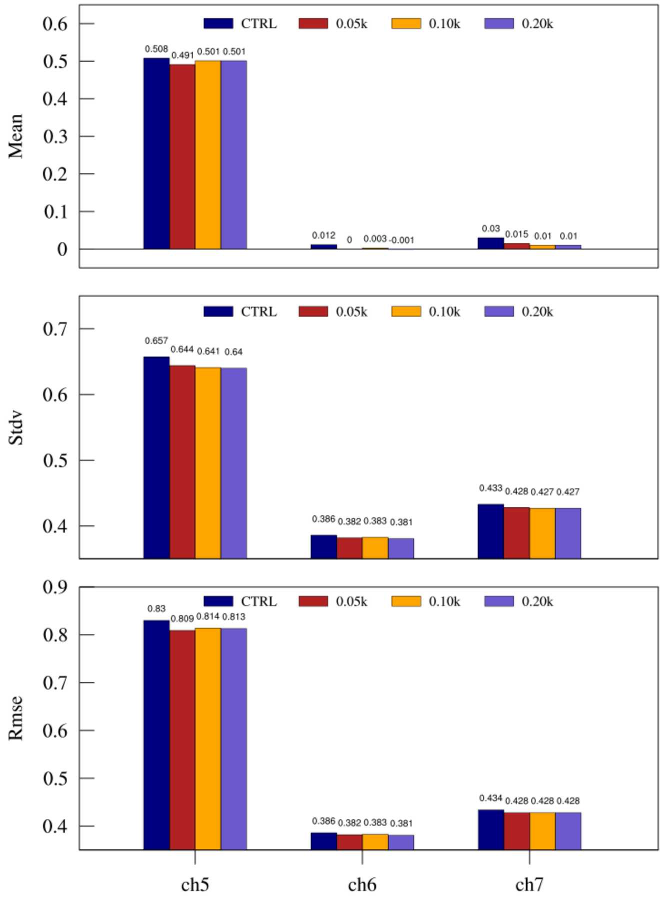


O-B to 3 channels

# Summery

1, RTTOV has been used in application of FY data at CMA with various version

2, Coefficients to RTTOV could be generated to sensors of FY satellite both in infrared  and in microwave at NSMC

3, Satisfied simulations to FY satellite by RTTOV could be obtained while comparisons are performed to radiance not only from LBL model, but also from observations

4, Pre-quality controls to MWTS have been used that is based on analysis to sensitivity between radiance and cloud parameters by RTTOV

# Future : AI in radiative transfer

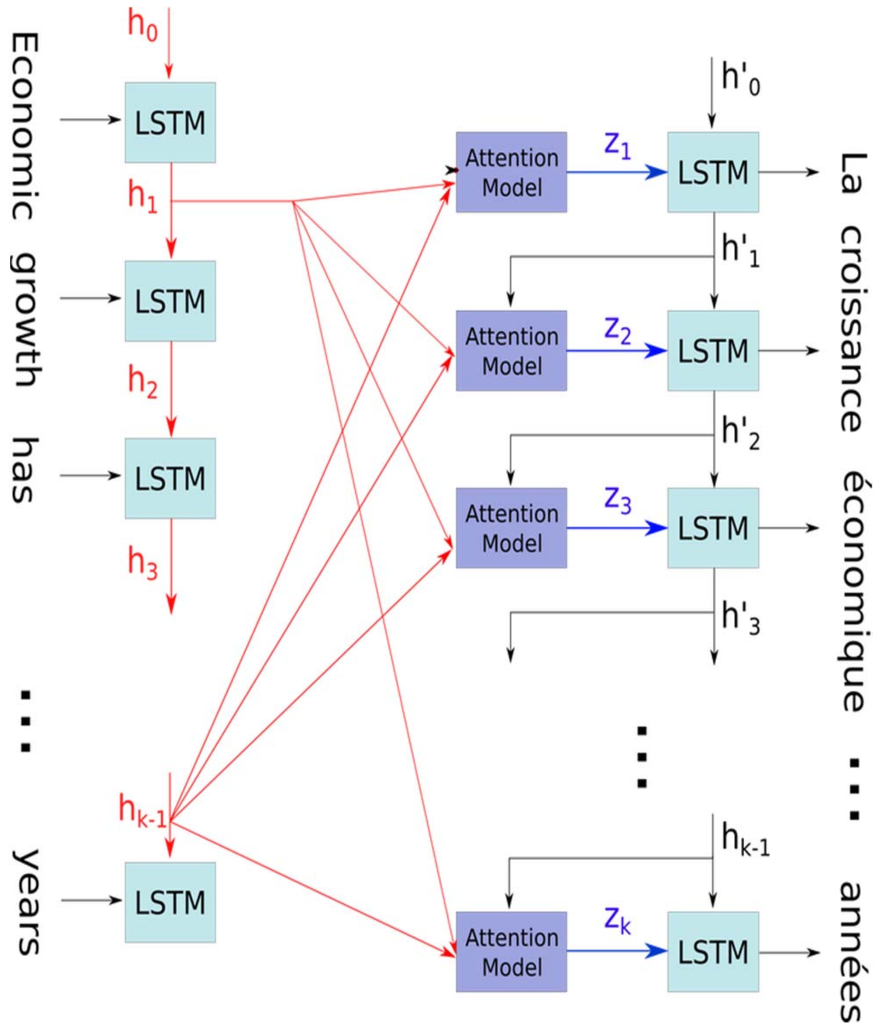


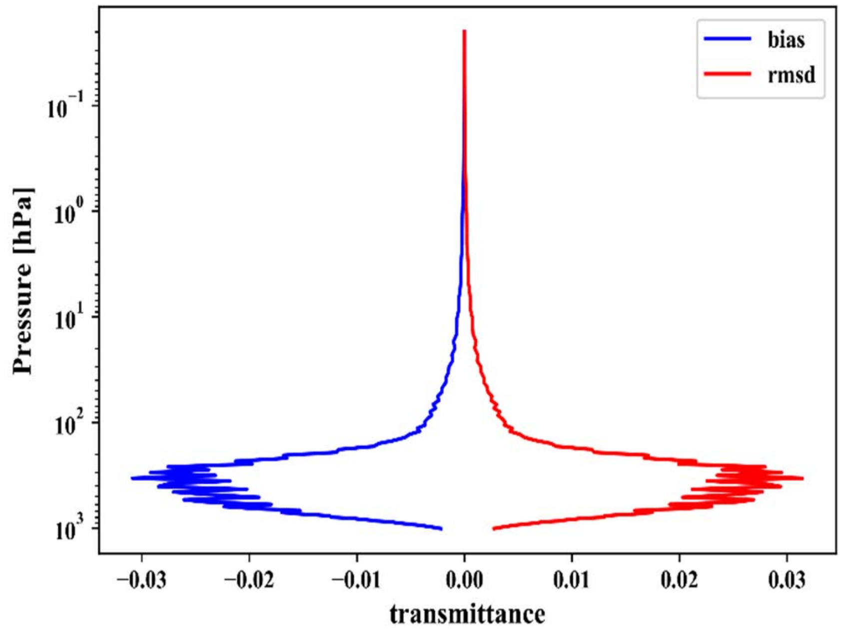


Deviation between AI and RTTOV

# Future : non-unfied training database

- Profiles dataset to training coefficients were classified by total water vapor content

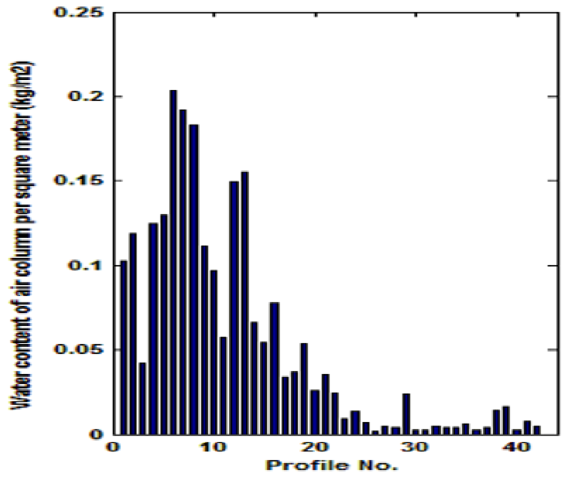


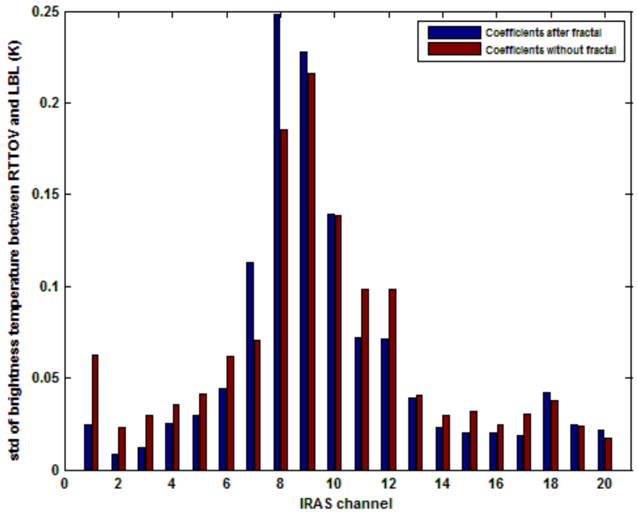


STD to wet profiles

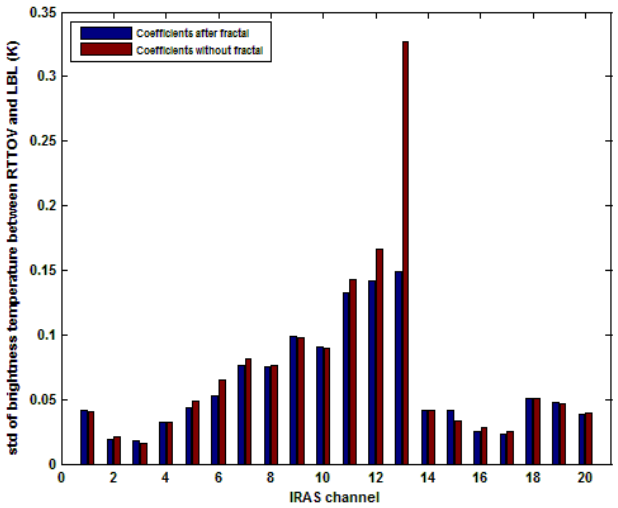


STD to dry profile

# Future : ray-tracing in radiative transfer calculation

$$R = \varepsilon \cdot B(T_s) \cdot \tau_s + \sum_{k=1}^{lev} \sum_{i=1}^{n\text{-}grids} B\left(T_{k,i}\right) \cdot \frac{\partial \tau_{k,i}}{\partial p} dp + (1-\varepsilon) \cdot \tau_s \sum_{k=1}^{lev} \sum_{i=1}^{n\text{-}grids} B\left(T_{k,i}\right) \cdot \frac{\partial \tau_{k,i}}{\partial p} dp$$

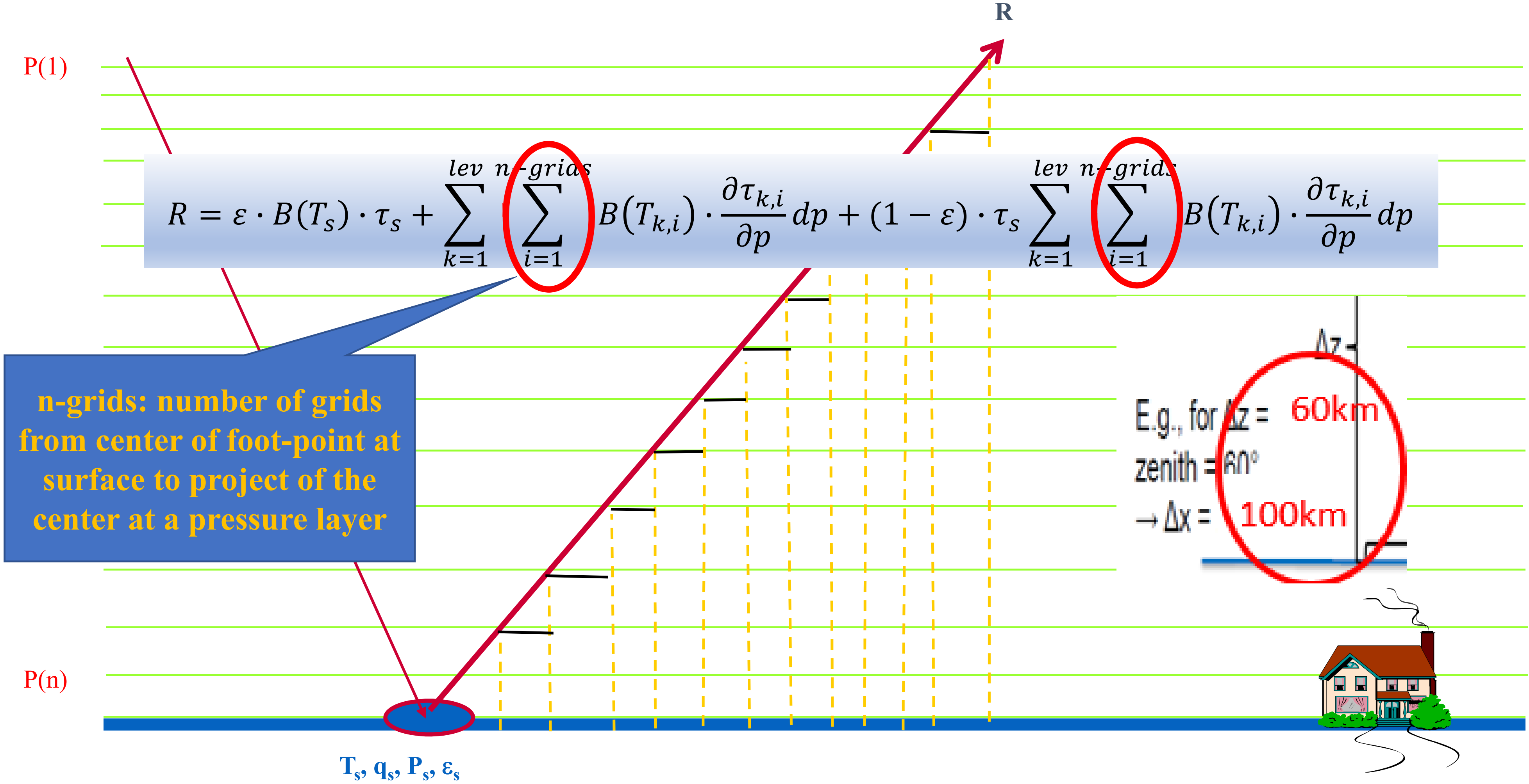

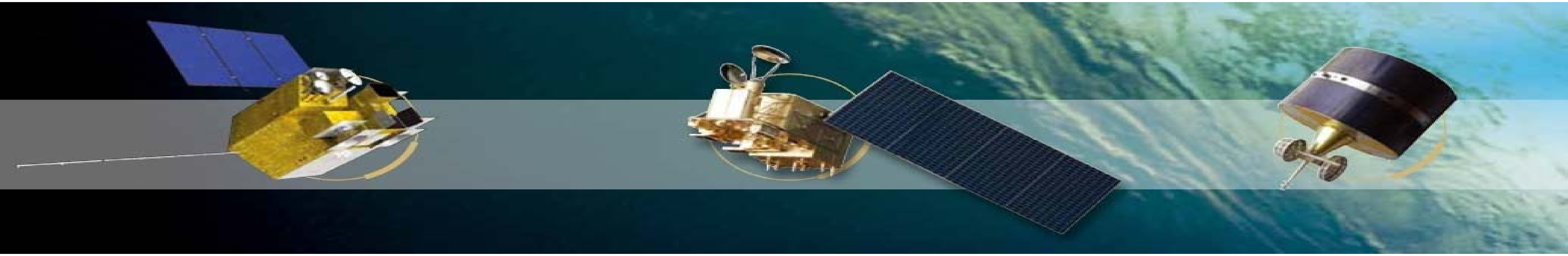

# *Thanks for your attention*